# Organic biomarker sea surface temperature proxies in Mediterranean Sea sediment traps

Sidney Bickerton

MSc thesis

Course code: GEO4-1520
ECTS: 45

Supervision: Addison Rice, Anouk van Boxtel, Francien Peterse

# Abstract

Paleoclimate proxies allow researchers to assess past climate and how it changed over time. Two sea surface temperature (SST) proxies, $TEX_{86}$ and $U^{k}_{37}$, are based on biomarkers called alkenones and glycerol dialkyl glycerol tetraethers (GDGTs), respectively. Specifically, $U^{k}_{37}$ is the degree of unsaturation of long-chain alkenones, and $TEX_{86}$ is based on the relative number of ring moieties in GDGTs. In the Mediterranean Sea, $TEX_{86}$ tends to overestimate SST by 2-6 ºC on average, while $U^{k}_{37}$ underestimates SST by 2-4 ºC when using calibrations based on globally distributed core tops. Examining these biomarkers in sinking particles collected by sediment traps can provide insight into why these offsets occur. Here, we study the potential impact of seasonality and possible biases in export on the $TEX_{86}$ and $U^{k}_{37}$ by analyzing alkenones and GDGTs in biweekly sediment trap material collected at 510 m, 1745 m, and 2920 m depth in the Urania Basin in the Eastern Mediterranean Sea from August 1999 until July 2000 and from August 2005 until July 2006. The results show a general agreement of the individual sediment traps using either paleotemperature proxy. Reconstructed temperatures of $TEX_{86}$ show little variation on an annual scale. A large influence of Deep Dwelling Thaumarchaeota is found to be a possible cause for a lack of seasonality and an annual overestimation of SST. The annual flux of GDGTs does show seasonality and peaks from late winter through early spring causing annual temperature predictions by $TEX_{86}$ to be weighted toward this time of the year. The long-chain alkenone flux peaks around the same time as the GDGT flux. The $U^{k}_{37}$ temperature prediction shows seasonality and correlates relatively well with SST during autumn and winter. During spring and summer, the $U^{K}_{37}$ signal better represents sub-mixed layer temperatures at 40 m depth. This is likely caused by the increasingly stratified water column in the Mediterranean at this time of the year forcing Haptophyte algae to migrate to deeper waters. Even though export biases are found for each proxy concerning the timing and depth causing offsets in the temperature predictions, both paleotemperature proxies are useful tools to reconstruct past environments. However, they are to be used with caution and awareness of the uncertainties that come with using them.

# Introduction

### *Climate Change and value of paleoreconstructions*

Reconstruction of past environments provides an opportunity to analyse climatic conditions on Earth through time. Sea surface temperature (SST) is a crucial parameter in palaeoceanographic studies and is used to estimate past environmental conditions (Huguet et al., 2010). Hence, paleotemperature reconstructions are implemented as input data for climate models used to project where temperatures are likely headed in the (near) future. The ability to predict paleo SST accurately allows for a more reliable prediction of future climate variability and its effect on environments globally. To understand climate variability, the ability to make accurate paleotemperature reconstructions is obligatory.

### *Proxies for SST and how they work*

Proxies are a tool in paleotemperature reconstructions that allow for a prediction of past climate conditions. Paleotemperature proxies often use a changing ratio between to factors to predict the environment over a certain timespan. Some of the more widely used proxies are $\delta^{18}O$, Mg/Ca, $U^k_{37}$ and $TEX_{86}$. $U^k_{37}$ and $TEX_{86}$ are palaeoceanographic SST proxies. For climate models to be reliable, these temperature proxies, and their seasonality should be well understood. To understand the proxy, the biomarker where it originates from, and its living conditions should be understood (Huguet et al., 2011; Rosell-Melé & Prahl, 2013; van der Weijst et al., 2022; Rice et al., 2022).

#### *$U^k_{37}$*

$U^k_{37}$ is a lipid biomarker paleotemperature proxy that is widely used across the world for different settings and timescales. It is based on the degree of unsaturation of long-chain alkenones produced by Haptophyte algae (Brassel et al., 1986a,b). Haptophyte algae are autotrophic organisms that live in surface waters in many settings across the world (Nicholls, 2015). In the Mediterranean Sea, Haptophyte algae synthesise long-chain alkenones mostly between 10 m and 40 m water depth (Cacho et al., 1999). A correlation between these long-chain alkenones and SST was initially introduced by Marlowe in 1984. Prahl et al. (1988) introduced the equation used in this report:

$$U^{k'}_{37} = [C_{37:2}] / [C_{37:2}] + [C_{37:3}] \quad \text{(Eq. 1)}$$

For the temperature calibration the equation from Muller et al. (1998) is used:

$$SST = (U^{k'}_{37} - 0.044) / 0.033 \quad \text{(Eq. 2)}$$

$C_{37:2}$ and $C_{37:3}$ refer to the varying number of unsaturations (2 double bonds, given as $C_{37:2}$ and 3 double bond, given as $C_{37:3}$). A higher SST results in a higher degree of unsaturation (Brassell et al., 1986).
$U^k_{37}$ and SST hold a global relationship through the calibration developed by Conte et al. (2006):

$$T = -0.957 + 54.293(U^{k'}_{37}) - 52.894(U^{k'}_{37})^2 + 28.321(U^{k'}_{37})^3$$

Here, an increased temperature leads to increased $U^k_{37}$ values (Conte et al., 2006). Earlier global calibrations have been developed on several occasions including by Prahl et al. (1988):

$$U^k_{37} = 0.034T + 0.039$$

Prahl et al. (1988) claim the absolute amount of long-chain alkenones produced per cell does not relate to temperature changes; only the ratio of the degree of unsaturation of long-chain alkenones changes with temperature, enabling it to predict SST.

### *$TEX_{86}$*

The TetraEther indeX of 86 carbons ($TEX_{86}$), is a proxy for SST (Schouten et al., 2002). $TEX_{86}$ is based on the relative abundance of cyclopentane and cyclohexane ring moieties in isoprenoid Glycerol Dialkyl Glycerol Tetraether (isoGDGT) lipids. This lipid forms a monolayer in the cell membrane of Thaumarchaeota, the major producers of isoGDGTs in pelagic marine environments (Schouten et al., 2013). Thaumarchaeotal isoGDGTs incorporated in $TEX_{86}$ can contain 0 to 4 cyclopentane rings, and are named GDGT-0 to GDGT-4, respectively. Then there is crenarchaeol and its stereoisomer: cren', which have an additional cyclohexane ring (Schouten et al., 2002; Sinninghe Damsté et al., 2002). Schouten et al. (2002) found that a higher abundance of ring moieties in the core structure of isoGDGTs present in marine surface sediments corresponds to a higher SST. Eq. 3, developed by Kim et al. (2010), takes the log of the ratio between different forms of GDGTs. Eq. 2 is developed by Kim et al. (2015) with the aim of calibrating $TEX_{86}$ to the Mediterranean:

$$TEX^{H}_{86} = \log([GDGT\text{-}2]+[GDGT\text{-}3]+[Cren']/[GDGT\text{-}1]+[GDGT\text{-}2]+[GDGT\text{-}3]+[Cren']) \quad \text{(Eq. 3)}$$

$$SST = 56.3 \times TEX^{H}_{86} + 30.2 \quad \text{(Eq. 4)}$$

Eq. 3 is regarded by Taylor et al. (2013) as a calibration appropriate for water depths >1000 m, i.e. the Urania Basin. Thaumarchaeota are nitrifiers found in all of Earth's oceans and seas at almost every water depth. However, they are most abundant below 50 m and above 500 m (Sollai et al., 2018). In the Mediterranean, they prefer subsurface waters below 100 m (Besseling et al., 2019, Fig.2). Typically, $TEX_{86}$-derived temperature estimates are based on isoGDGTs in marine surface sediments (reference surface sediment studies and core-top studies).

Despite successful reconstructions, two proxies seem to predict SST less accurately in the Mediterranean Sea compared to elsewhere. Theories of the cause of these issues have been published but the answer remains unclear (Kim et al., 2010; Tierney & Tingley 2014).

### *$U^{k}_{37}$ uncertainties*

According to Ternois et al. (1997) and Tierney & Tingley (2018), seasonality has proven to have substantial influence on the reliability on $U^{k}_{37}$ as a temperature proxy, where $U^{k}_{37}$ correlates best with SST when alkenone production is highest. Above 24 ºC, $U^{k}_{37}$ sensitivity to temperature change decreases, and above 28 ºC, $U^{k}_{37}$ is saturated, i.e., only $C_{37:2}$ alkenones are present, making it impossible to predict SST using this proxy (Tierney & Tingley, 2018).
The global calibration model from Conte et al. (2006) has a standard error of 1.2 ºC. Global trends show that data lying between 10-25 ºC is the most linear section of the response function (Conte et al., 2006). Conte et al. (2006) found that core-top $U^{k}_{37}$ data from the Pacific and Atlantic Ocean is consistently higher than the surface water $U^{k}_{37}$ for temperatures below 22 ºC. For the North Atlantic Ocean, Tierney & Tingley (2018) found the highest correlation between $U^{k}_{37}$ and SST in April and the lowest in February. In the North Pacific Ocean, the highest correlation was in June, July and August and the lowest in September.
In the Mediterranean Sea, Haptophyte algae synthesise long-chain alkenones mostly between 10 m and 40 m water depth (Cacho et al., 1999). Their concentration is strongly dependent on the time of the year, and $U^{k}_{37}$ correlates best with November to May SSTs

(Ternois et al., 1996). $U^{k}_{37}$ calibration executed by Ternois et al. (1996) in the northwestern Mediterranean underestimates SST on an annual scale. However, in this research, the sediment trap record misses the warmer summer months. In spring, the Mediterranean is characterised by spring blooms in which Haptophyte algae are not the major phytoplanktonic species (Ternois et al., 1997). During these months, the creation of a thermocline takes place and surface waters are slowly being depleted (Cacho et al., 1999). Tierney & Tingley (2018) measured the highest correlation between $U^{k}_{37}$ and SST during the winter and the lowest during summer, when stratification is highest. They also find a consistent underestimation of SST by $U^{k}_{37}$ of 2-4 ºC. However, it remains unclear what exactly causes the underestimation of SST in the Mediterranean when using $U^{k}_{37}$ as a paleothermometer. This Mediterranean offset is analysed in this research with the aim of making $U^{k}_{37}$ a more reliable proxy for future paleotemperature research. This is done by studying the annual long-chain alkenone flux and identifying how it relates to the proxy signal. The $U^{k}_{37}$ signal is compared to sub-mixed layer temperatures in the water column to analyse the export depth of long-chain alkenones. The influence of varying production trends at different depths in the water column and the possibility of a seasonal bias will be studied in this research to assess the reliability of using $U^{k}_{37}$ as a paleothermometer.

### *$TEX_{86}$ uncertainties*

It remains unclear from what exact depth in the water column the $TEX_{86}$ signal in surface sediments mainly originates. The GDGT-producing community composition varies with depth (Taylor et al., 2013; Besseling et al., 2019). Through studying the genome involved in ammonia oxidation, Francis et al. (2005) and Hallam et al. (2006) found a distinct difference between surface populations of Thaumarchaeota and deep-water populations, categorising them as different ecotypes. The ratio of GDGT-2/GDGT-3 (2/3-ratio, hereafter) will, be explored in this project as it provides insight into the influence of deep-water Thaumarchaeota and the export depth of GDGTs (Besseling et al., 2019). Sedimentary GDGT-2/GDGT-3 ratios are positively correlated with the overlying water depth. Through studying surface sediments, Deep-dwelling Thaumarchaeota communities have a high GDGT-2/GDGT-3 ratio and are incorporated in suspended particulate matter (SPM), however to what degree on an annual scale remains unclear (Taylor et al., 2013).
With increasing water depths, GDGT-2 concentrations increase while GDGT-3 decreases. Higher ratios occur with increasing water depth (Taylor et al., 2013). This potentially means, according to Taylor et al. (2013), that differences in GDGT distributions ascribed to temperature could instead be related to the depth of the water mass overlying the sediment. This research is based on sedimentary GDGT distributions and core-top data. Measuring GDGT-2/GDGT-3 ratios from annual sediment trap samples could provide insight in potential seasonal trends in this ratio and the $TEX_{86}$ signal. When the GDGT-2/GDGT-3 ratio is >5, there is a greater chance of GDGTs originating from Thaumarchaeota populations living in deep water settings dominating the $TEX_{86}$ signal, so called deep-dwelling Thaumarchaeota. If the GDGT-2/GDGT-3 ratio is <5, there is a greater chance of Thaumarchaeota living in surface waters dominating the $TEX_{86}$ signal (Taylor, et al., 2013; Hernández-Sánchez, et al., 2014). In the Mediterranean, the GDGT-2 concentration, and the GDGT-2/GDGT-3 ratio, increases with increasing water depth (Besseling et al., 2019). However, a deep-water setting (>1000 m) does not guarantee a high GDGT-2/GDGT-3 ratio. 29% of global deep-water settings still exhibit a GDGT-2/GDGT-3 ratio <5.
The depth of the water column influences the export depth of GDGTs. The Urania Basin is over 3500 m deep and is, therefore, considered a deepwater setting (Sass et al., 2001; Taylor et al., 2013). Taylor et al. (2013) suggests that in these settings, $TEX_{86}$ values in core-top sediments show contribution from subsurface waters, even though they have been calibrated against SST. The $TEX_{86}$ signal from this research will, therefore, be compared to both SST and subsurface temperatures at different depths.
The ratio of GDGTs relies on the export depth and timing of GDGTs in the water column. The production depth of GDGTs likely relates to the nitracline, however, this is not equal to the export depth of GDGTs (Mollenhauer, et al., 2008). GDGTs are neutrally buoyant and

cannot sink by themselves. The export depth can differ from the depth they are produced at (Iversen & Ploug, 2010; Mollenhauer et al., 2015). Therefore, the export timing of GDGTs varies based on Net Primary Production (NPP). NPP enhances faecal packaging mostly in surface waters as this is where zooplankton live. Therefore, GDGTs from surface waters are more effectively exported than deep water GDGTs when NPP is relatively high (Wuchter et al., 2005).

In the Mediterranean Sea, $TEX_{86}$ has a warm bias of 2-6 degrees Celsius (Kim et al., 2015, 2016). In order to explain this offset, and to increase the reliability of $TEX_{86}$-paleothemometry, it is crucial to understand the difference in isoGDGT distributions produced at different depths in the water column. Kim et al. (2015) found a deep-water dwelling Thaumarchaeota community in the Mediterranean Sea. This community produces warmer $TEX_{86}$-derived SST compared to surface-dwelling populations. They state that there is an increase in GDGT-2 and cren' with depth, together with a decrease of GDGT-1 and GDGT-3, which Besseling et al. (2019) confirm. For this reason, Kim et al. (2015) make a deep-water $TEX_{86}$ calibration for surface sediments of >1000 m water depth in the Mediterranean. This calibration correlates better to mean annual SST than the global core-top calibration developed by (Kim et al., 2010; eq. (3)). However, it is not enough to eliminate the offset to mean annual SST in the Mediterranean. Another point of discussion is whether $TEX_{86}$ is related to SST or to subSST. Thaumarchaeota have a preference for subsurface waters (Sollai et al., 2018). Ho & Laepple (2016) found that changing the target temperature for $TEX_{86}$ calibrations from SST to subSST leads to decreased amplitude of change and an overall decrease in $TEX_{86}$-inferred temperatures. This does not explain the depth origin of GDGTs exported to surface sediments, yet it does prove the importance of choosing the right target temperature for $TEX_{86}$ calibrations to accurately reconstruct past climate.

Kim et al., 2015, finds that the $TEX_{86}$ signal in the Mediterranean cannot solely be influenced by annual mean SST. Other environmental factors likely influence the signal and the export mechanisms of GDGTs. For instance, Tierney & Tingley (2014) found that, on a global scale, lower nutrient availability leads to $TEX_{86}$ having an increased sensitivity to temperature change, which will be investigated in this report. Seasonality, will also be investigated to see if the offset concerning $TEX_{86}$ is more predominant during certain seasons. Seasonality has been studied and consequently dismissed as a major cause of the bias by Kim et al. (2015) and Tierney & Tingley (2014). However, these researches used box- and multi-corers and sediment coretops, respectively. Using sediment traps could give new insight in the time of production and export of GDGTs and with that, clarify if seasonality is in fact a factor to be dismissed when studying the Mediterranean offset of $TEX_{86}$ SST predictions.

### *Aims and Approach*

This research aims to analyse the influence of environmental mechanisms on production patterns of GDGTs in the Urania Basin. The Mediterranean offset concerning $TEX_{86}$ SST predictions is assessed by studying seasonal patterns of the flux and the export depth of GDGTs. Just like for $U^k_{37}$, the $TEX_{86}$ signal is compared to sub-mixed layer temperatures to analyse annual proxy trends.

In this research, annual trends of environmental conditions surrounding Haptophyte algae and Thaumarchaeota are compared to their seasonal flux and how this relates to the SST predictions of the corresponding proxy. The aim of this is to understand better the output signal of both proxies and why certain offsets occur in the Mediterranean.

Concerning $U^k_{37}$ and $TEX_{86}$, a lot of research is done by using surface sediments and core-top calibrations. This way you get a summary of the biomarkers of the entire overlying water column and of several years. Using sediment traps, a detailed record of the seasonal pattern

of each proxy can be revealed. Sediment trap research has been performed before in the Mediterranean, however, not using several sediment traps at different depths in the same location. By comparing sediment traps at different depths, production and export trends of the biomarker can be analysed. A comparison of biomarker distributions across different water depths can be made. Seasonal trends concerning several environmental factors will be considered for a reliable comparison with the biomarker export and proxy signal.

Specific questions that will be adressed are:

- *What trends in fluxes of GDGTs and long-chain alkenones can be identified across one year and how does the sampling year of 1999/2000 compare to 2005/2006?*
- *What trends concerning temperature predictions of both biomarkers are visible across one year of samples?*
- *How do SSTs based on $TEX_{86}$ and $U^{k}_{37}$ compare to SSTs retrieved from satellite imagery?*
- *How do the GDGT and long-chain alkenone ratios change with depth?*
- *What environmental mechanism is driving the export of GDGTs and long-chain alkenones from the different depths in the water column to the seafloor?*

Using $TEX_{86}$ and $U^{k}_{37}$, SSTs are estimated and compared to satellite-based SSTs from the corresponding year. The proxy results will also be compared to each other as well as between sampling years and possible seasonal trends will by identified. The proxy SST estimations are also compared to NPP and, more specifically, phosphorus, nitrate, and oxygen concentration throughout the year and at different depths in the water column. The results of the 3 sediment traps are individually compared to SST measurements and surface sediment calibrations from previous literature to test which has the highest correlation to SST. This will help clarify the significance of changing Thaumarchaeota and Haptophyte algae community composition with depth. It can furthermore lead to a better understanding of the export mechanisms of GDGTs and long-chain alkenones to the seafloor, and which environmental factors force the size and timing of these vertical fluxes. The aim of this project is to constrain the most likely export depth of these biomarkers, and to understand their export mechanisms to the seafloor. This will strengthen the reliability of assessing SST using $TEX_{86}$ and $U^{k}_{37}$ as paleothermometers. The influence on the paleotemperature measurements of environmental factors like seawater stratification and nutrient concentration in the water column will be investigated for the Urania Basin. In this way, they can be used more reliably to predict the SST in the Mediterranean of current and past environments.

# Materials & Methods

### *Study area*

The Mediterranean is known to be oligotrophic throughout most of the year. There is a limitation of phosphorus restraining primary productivity (Krom et al., 1992). There is an overall low primary productivity when compared to the Atlantic Ocean (Civitarese et al., 2010). Stratified water masses have a major influence on the productivity of the Mediterranean. Modified Atlantic Water (MAW) entering the Mediterranean through the straight of Gibraltar lies on top of Levantine Intermediate Water (LIW) which is formed in the Levantine Basin in the eastern Mediterranean. LIW is more saline and denser than MAW, preventing vertical mixing which leads to oligotrophic conditions (Besseling et al., 2019; Tanhua et al., 2013). SST increases from west to east in the Mediterranean (Rice, 2022). Strong seasonality in temperature and thermocline depth is found throughout the

Mediterranean (Civitarese et al., 2010). Summer is characterised by strong stratification. The sea surface temperature is highest from August to September when the surface mixed layer is most shallow. Vertical mixing starts in September and reaches its peak in January (Malinverno et al., 2009). Mixing of the water column is partly caused by wind stress, which in combination with precipitation induces wet Saharan dust deposition that fertilises the upper water column (Krom et al., 1992). Using satellite imagery, pigment concentration of the surface waters of the Mediterranean can be measured and used to determine NPP.

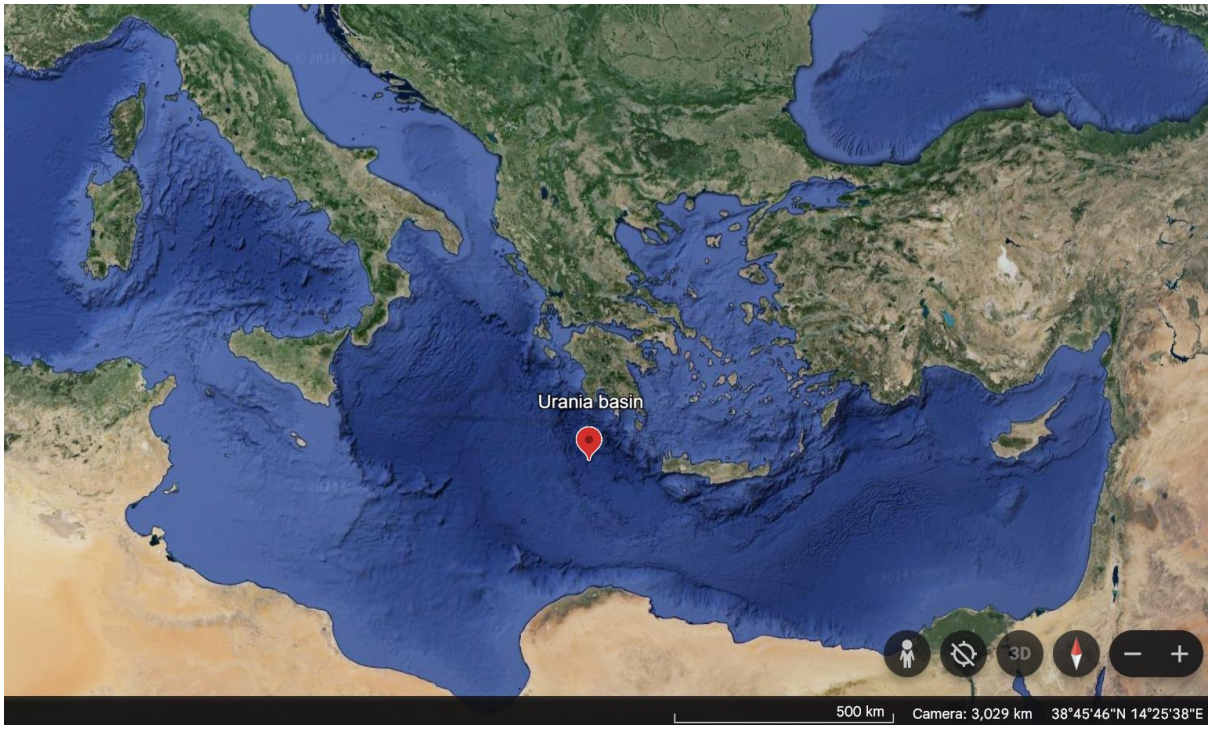

Fig. 1: Location of the sediment traps.

Urania Basin is located in the central-eastern Mediterranean. This area is productive from December to March when the mixed surface layer is deepest (Ziveri et al., 2000). The Urania Basin has a low input of organic matter of terrestrial origin compared to surrounding areas in the Mediterranean (Polymenakou et al. 2007). Saharan dust input does likely influence organic matter concentration in the Urania Basin during certain seasons (Ternon, et al., 2010).

Material is collected by sediment traps placed in the Urania Basin in the eastern Mediterranean Sea at 3 different depths: 510 m, 1745 m, and 2920 m. All sediment traps were located above the seawater/brine interface in oxygenated conditions (Rutten et al., 2000). Specifically, material collected by these traps every 2 weeks for 2 different years, i.e., from 15/09/1999 to 13/05/2000 and from 12/09/2005 to 23/08/2006 was analysed in the laboratory at the University of Utrecht.

### *Lipid biomarker analysis*

In total 138 were selected for lipid extraction. All samples were filtered onto glass fibre filters, freeze-dried and subsequently weighed. To extract all organic lipids from the samples, they were microwaved in 25 mL DCM:MeOH 9:1. The extract were poured into 40 mL vials and rinsed twice with 5 mL DCM:MeOH 9:1. Using a TurboVap they were blown down until 1-2 mL remains which was then run through a $NaSO_4$ column using DCM:MeOH 9:1 and dried under $N_2$. Acid hydrolysis was performed using 0.5 mL 1.5N HCl and reacted at 70 °C for two hours. 0.5 mL MilliQ was added to each TLE vial after it had cooled. Liquid-liquid extraction

was performed using DCM and the extract was put through a $NaSO_4$ column using DCM:MeOH 9:1.

Methylation was then performed by adding 0.5 mL DCM:MeOH 1:1 which dissolves the sample. 10 µL 0.2 M diazomethane was added. After 30 minutes, 10 µL 0.2 M acetic acid was added and dried under $N_2$. The sample was then passed over a column of non-activated silica gel with a small amount of $Na_2CO_3$ to neutralize the acid using ethyl acetate and dried under $N_2$.

The dissolved samples was then separated into 3 fractions using an aluminum oxide column and eluted with hexane:DCM 9:1 for an apolar fraction, hexane:DCM 1:1 for a neutral fraction and DCM:MeOH 1:1 for a polar fraction. They were dried under $N_2$ and weighed. To prepare the neutral samples heavier than 0.5 µg for gas chromatography, 50 µL ethyl acetate was added per 0.1 µg sample. For neutral samples <0.5 µg, 25 µL ethyl acetate was added for the upper sediment traps and 10 µL for the lower sediment traps.
To quantify the isoGDGTs, an internal GDGT standard was added to the polar fraction and dried under $N_2$ before dissolution in 500 µL 99:1 hexane:IPA for the upper sediment trap samples and 250 µL for the lower traps. The sample was then put through a 0.2 µm filter using a syringe. The filtered sample was added to a 1.5 mL vial.

Long-chain alkenones were analysed using a Hewlett Packard 6890 series gas chromatograph. 1 µL of the neutral sample, containing the long-chain alkenones was co-injected with 1 µL of squalene standard in the gas chromatograph equipped with a 30 m CP-Sil 5 CB column. The filtered polar fraction of the sample was injected in an Agilent 1260 Infinity ultra-high-performance liquid chromatographer coupled to an Agilent 6130 single quadrupole mass detector. The C37 and GDGT peaks, given by the GC and LC, were identified by comparing retention times with standard chromatograms. They were then manually integrated with Agilent Chemstation 32 using the m/z in table 1.

Table 1. Type m/z corresponding to the type of GDGT used for peak integration

| *m/z* | 1302 | 1300 | 1298 | 1296 | 1292 | 1292 |
|---|---|---|---|---|---|---|
| *GDGT* | GDGT-0 | GDGT-1 | GDGT-2 | GDGT-3 | Cren | Cren’ |

From this data, the results were produced using Eq. 1 and Eq. 2 for $U^k_{37}$ and Eq. 3 and Eq. 4 for $TEX_{86}$. The biomarker mass flux was calculated by comparing the peak area of the biomarkers and its dilution with the amount of internal standard injected and its peak area.

Apart from SST, the proxy signals were compared to sub-surface temperatures at 30 m, 40 m, 55 m, 100 m, and 200 m depth obtained from satellite data collected by the Copernicus Marine Service, Global Ocean Physics Reanalysis.

The results were also compared to annual phosphate, nitrate, and oxygen concentrations and NPP which are sourced from Copernicus Marine Service, Global Ocean Biogeochemistry Hindcast. Graphs produced for this research were plotted using MATLAB R2022b. These graphs include the environmental factors listed above, showing their concentration at different depths on an annual scale. The proxy signals were plotted on the same scale for each sediment trap. Additionally, the biomarker flux was calculated and plotted the same way.

# Results

*Long-chain alkenone fluxes and indices*

In 1999/2000, the sediment trap 1 has an average flux of 0.5 µg/m$^2$/day. Sediment trap 2 is 0.04 µg/m$^2$/day on average and sediment trap 3, 0.06 µg/m$^2$/day. The flux of all three sediment traps ranges from 0.0014 to 2.0 g/m$^2$/day. Sediment trap 1 shows the largest variance for both years. In 2005/2006 the average long-chain alkenone flux is 0.13 µg/m$^2$/day. Sediment trap 1 has the highest average flux with 0.32 µg/m$^2$/day. Sediment trap 2 has an annual average flux of 0.02 µg/m$^2$/day and sediment trap 3 is 0.05 µg/m$^2$/day. The long-chain alkenone flux during 1999/2000 is 0.06 µg/m$^2$/day higher on average than the flux during 2005/2006 (Fig. 2).

For both sampled years from December to February, sediment trap 1 has a relatively low alkenone flux, 0.32 µg/m$^2$/day in 1999/2000 and 0.15 µg/m$^2$/day in 2005/2006, being 0.16 µg/m$^2$/day and 0.17 µg/m$^2$/day lower than their respective annual averages (Fig. 2). Sediment trap 1 in 1999/2000 experiences a higher alkenone flux from September through November and during February. A maximum flux of 1.99 µg/m$^2$/day is reached in mid-November and is twice as high as the second highest value measured that year. 2005/2006 has a higher alkenone flux from March through June and reaches a maximum of 0.77 µg/m$^2$/day in March. The higher fluxes measured in sediment trap 1 in November 1999 and in October 2005 are almost completely caused by a C37-2 flux. The rest has a similar contribution of both C37-3 and C37-2 alkenones. The extent of variation found in sediment trap 1 is lacking in the other sediment traps for both years. Sediment trap 3 in 1999/2000 reaches a maximum flux of 0.17 µg/m$^2$/day in February and one month later in March a maximum alkenone flux of 0.18 µg/m$^2$/day is reached sediment trap 2. In 2005, sediment trap 2 shows a maximum long-chain alkenone flux in November of 0.10 µg/m$^2$/day. The long-chain alkenone flux in sediment trap 3 increased in February and reaches a maximum in March 2006 of 0.28 µg/m$^2$/day. Apart from these moments, the flux trends of sediment traps 2 and 3 are reasonably constant compared to the trend of sediment trap 1 for both years (Fig. 2).

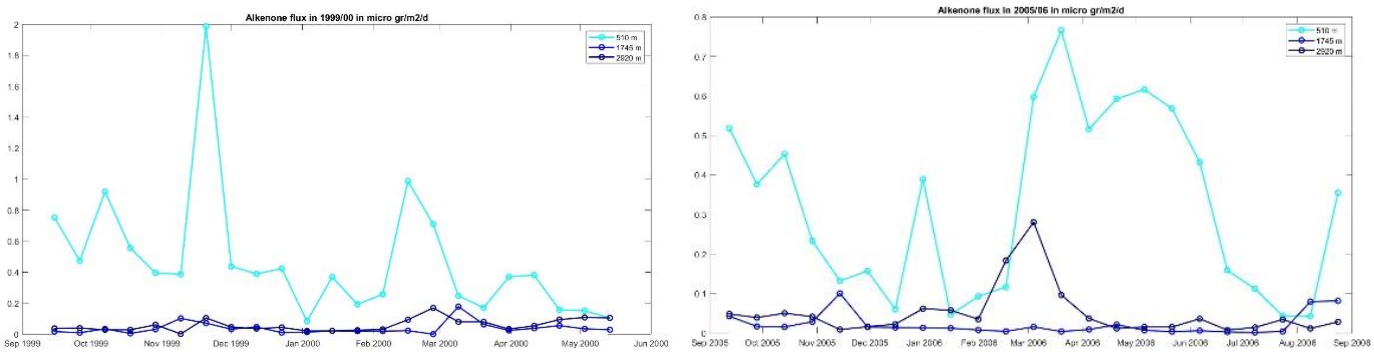


Fig. 2: Flux of C37 alkenones for each sediment trap in µ gr/m$^2$/day.

The flux weighted average calculates the $U^k_{37}$ signal using the sum of the C37:3 and C37:2 flux for each sediment trap. It allows for an expectation of the $U^k_{37}$ SST prediction in the underlying surface sediment on an annual scale. Sediment trap 1 predicts the highest $U^k_{37}$ surface sediment signal and sediment trap 3 the lowest. The flux weighted average of

sediment trap 1 is closest to the $U^k_{37}$ signal measured during summer. Sediment trap 2 and 3 are closest to the $U^k_{37}$ signal measured in winter and spring.

Table 2. Flux weighted average $U^k_{37}$ per sediment trap and predicted SST.

| **Depth** | **$U^k_{37}$** | **SST** |
|---|---|---|
| *510 m* | 0.69 | 19.7 ºC |
| *1745 m* | 0.64 | 18.1 ºC |
| *2920 m* | 0.58 | 16.2 ºC |

### *$U^k_{37}$ SST prediction*

The difference between the minimum and maximum $U^k_{37}$ predicted SST is 13.3 ºC in 1999/2000 and 13.6 ºC in 2005/2006 (Fig. 6). For both years, $U^k_{37}$ predicts the lowest SST in spring, followed by winter, summer and the highest $U^k_{37}$ SST prediction is in autumn. Satellite SST has a different order with winter having the coldest SST, followed by spring, autumn and summer (Table 3).

Table 3. Average $U^k_{37}$ SST per season for 1999/2000 and 2005/2006 compared to average satellite SST per season.

| | $U^k_{37}$ SST 1999/2000 | Satellite SST 1999/2000 | $U^k_{37}$ SST 2005/2006 | Satellite SST 2005/2006 |
|---|---|---|---|---|
| Autumn | 22.4 ºC | 22.7 ºC | 21.5 ºC | 22.2 ºC |
| Winter | 17.2 ºC | 16.5 ºC | 16.6 ºC | 16.0 ºC |
| Spring | 16.0 ºC | 17.2 ºC | 14.5 ºC | 18.7 ºC |
| Summer | 22.4 ºC | 25.9 ºC | 16.5 ºC | 25.9 ºC |

In 1999/2000 the $U^k_{37}$ signal from all traps varies between 13.5 ºC and 26.5 ºC. In 2005/2006 the lowest and highest $U^k_{37}$ predicted temperatures are 11.9 ºC and 25.4 ºC (Fig. 3). From May onwards in 2006, the $U^k_{37}$ signal underestimates SST. An underestimation is also relevant from September until mid-November in 1999 and from September to mid-October in 2005. On average, the $U^k_{37}$ signal predicts a SST of 19.1 ºC in 1999/2000, which is 0.4 ºC higher than the satellite derived SST of that year, being 18.7 ºC on average. For 2005/2006 the average annual SST predicted using $U^k_{37}$ is 18.0 ºC and the satellite derived SST for that year is 20.00 ºC. When only considering the dates in 2005/2006 where there is also data for in 1999/2000, the average satellite SST is 18.4 ºC and the average $U^k_{37}$ predicted SST is also 18.4 ºC. Only considering the dates for which there is data in both years, satellite derived SST decreases with 0.3 ºC and the $U^k_{37}$ signal decreases with 0.7 ºC.

Comparing the satellite SST signal per season to the corresponding $U^k_{37}$ signal, yet still combining all 3 sediment traps, in 1999/2000 $U^k_{37}$ best predicts SST in autumn with an underestimation of 0.3 ºC. Winter comes in second with an overestimation of SST of 0.7 ºC, then spring where $U^k_{37}$ underestimates SST by 1.2 ºC. The worst prediction of SST by $U^k_{37}$ is in summer with an underestimation of 3.5 ºC.

For 2005/2006, the $U^k_{37}$ SST measurements during winter are closest to satellite SST of that season, overestimating them by 0.6 ºC on average. Second closest is during autumn with an underestimation of 0.7 ºC. During spring and summer, $U^k_{37}$ underestimates satellite SST with 4.2 ºC and 9.4 ºC, respectively (table 3).

a.

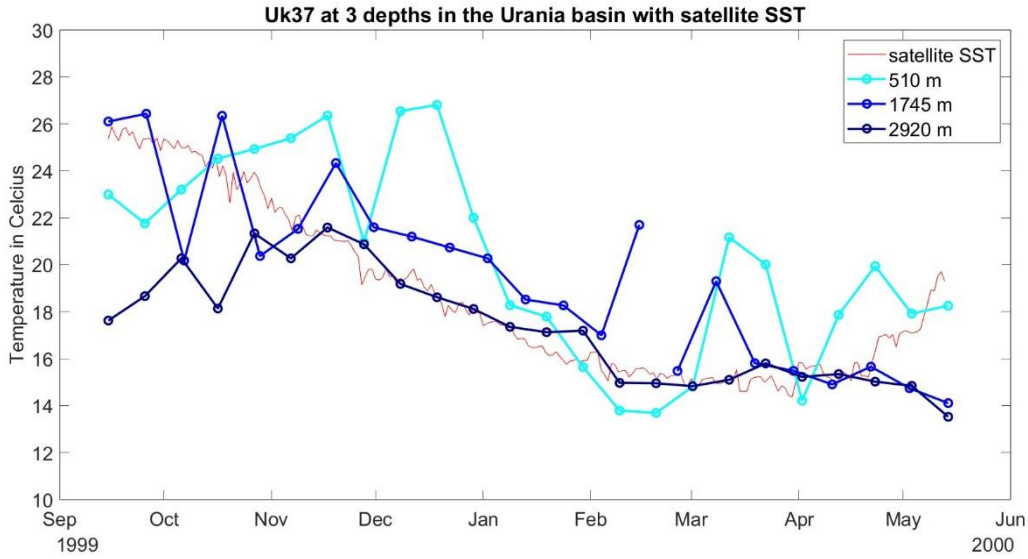


b.

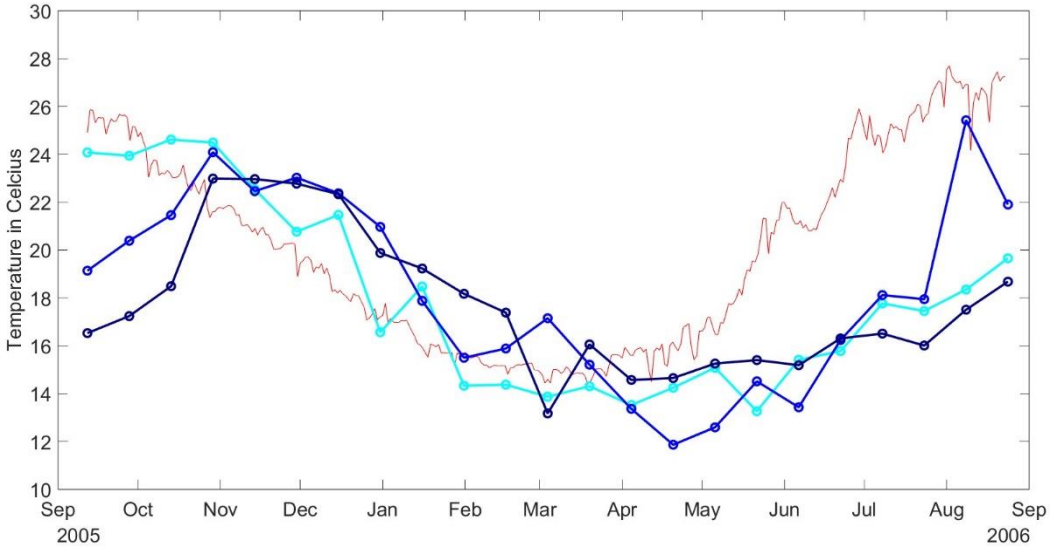


Fig. 3: SST estimates (using Eq. 2) derived from $U^{k}_{37}$ (using Eq. 1) from 3 sediment traps with satellite derived SST. (a.) 15/09/1999 to 13/05/2000. (b.)12/09/2005 to 23/08/2006.

### *GDGT fluxes and indices*

The flux of GDGTs to each sediment trap is measured in µg/m$^2$/day (Fig. 4). During 1999/2000, sediment trap 1 has an average flux of 314 µg/m$^2$/day. Sediment trap 2 has an average flux of 58 µg/m$^2$/day and sediment trap 3 of 81 µg/m$^2$/day. The annual average flux of sediment trap 1 in 2005/2006 is 165 µg/m$^2$/day, sediment trap 2 is 23 µg/m$^2$/day and sediment trap 3 is 43 µg/m$^2$/day on average. During 2005/2006, the total flux of all sediment traps is 73 µg/m$^2$/day lower on average than the first year.

During the last 2 weeks of November 1999, the GDGT flux of sediment trap 1 increases with 551 µg/m$^2$/day. During December 1999, the GDGT flux of sediment trap 1 decreases with 487 µg/m$^2$/day. From January until March 2000, it increases with 570 µg/m$^2$/day, when it

reaches the annual maximum of 718 µg/m$^2$/day. After this, the sediment trap 1 GDGT flux decreases until the end of April with 652 µg/m$^2$/day.

In January 2005/2006, the GDGT flux increases with 153 µg/m$^2$/day and subsequently decreases with 124 µg/m$^2$/day. That same year, from March to May, the GDGT flux increases with 528 µg/m$^2$/day when it reaches the annual maximum flux of 560 µg/m$^2$/day. The GDGT flux subsequently decreases until the last sampling point with 535 µg/m$^2$/day.

The maximum GDGT flux in 1999/2000 is reached roughly two months earlier, in March, than in 2005/2006, in May. Sediment trap 1 has a larger range of GDGT flux compared to sediment trap 2 and 3 which show less variation. In the first sampling year, they both have a maximum flux in September 1999 being 148 µg/m$^2$/day and 153 µg/m$^2$/day higher than their respective annual averages. For sediment trap 2, this is also the case in the second sampling year with September showing an average flux 122 µg/m$^2$/day higher than the annual average of sediment trap 2. In this year, sediment trap 3 has the highest flux from the second half of February through March being 62 µg/m$^2$/day higher than the annual average of sediment trap 3.

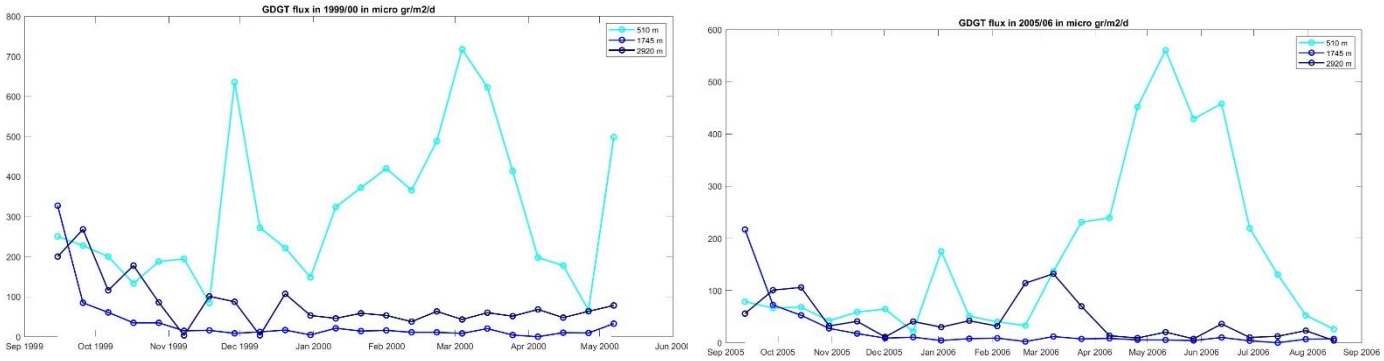


Fig. 4: Flux of GDGTs for each sediment trap in µ gr/m$^2$/day.

The flux weighted average calculates the $TEX_{86}$ signal using the sum of mass flux per sediment trap. It portrays the expected surface sediment on an annual scale.

Table 4. Flux weighted average $TEX_{86}$

| Depth | $TEX_{86}$ | SST |
|---|---|---|
| 510 m | 0.70 | 21.4 ºC |
| 1745 m | 0.73 | 22.5 ºC |
| 2920 m | 0.74 | 22.7 ºC |

### *$TEX_{86}$ SST prediction*

The $TEX_{86}$ signal shows little to no seasonality (Fig. 5). In the year 1999/2000, the $TEX_{86}$ signal of the 510 m sediment trap varies between 21.1 ºC and 22.4 ºC with an average temperature of 22.0 ºC. Sediment trap 2 varies between 22.2 ºC and 23.2 ºC with an average of 22.7 ºC. Sediment trap 3 varies between 22.2 ºC and 23.8 ºC with an average of 23.0 ºC. This means that the signal of all sediment traps has a range of 2.7 ºC, which is smaller than the range predicted by $U^{k}_{37}$. The deepest sediment trap predicts the highest temperatures, and that the shallowest sediment trap predicts the lowest temperatures on average.

The annual average of $TEX_{86}$ in 1999/2000 overestimates satellite derived SST by 3.9 ºC. The annual average of $TEX_{86}$ during 1999/2000, combining the results of all 3 sediment traps, represent autumn SST best with an overestimation of 0.7 ºC.
Similar results appear during 2005/2006 as the annual average $TEX_{86}$ predicted SST is closest to autumn SST with an overestimation of 0.6 ºC. On average in 2005/2006 $TEX_{86}$ overestimates annual SST by 1.6 ºC.

The $TEX_{86}$ signal of the year 2005/2006 shows a higher variance compared to 1999/2000. During February 2006, the $TEX_{86}$ signal of the three sediment traps decreases with 2.3 ºC on average with the smallest decrease in sediment trap 3. The predicted SST subsequently increases in March. The 510 m sediment trap has a range between 19.5 ºC and 22.1 ºC and an average temperature of 21.0 ºC. The 1745 m sediment trap ranges between 19.1 ºC and 22.6 ºC with an average temperature of 21.7 ºC. The 2920 m sediment trap shows the lease amount of variance ranging between 21.2 ºC and 22.9 ºC with and average temperature of 22.3 ºC.

a.

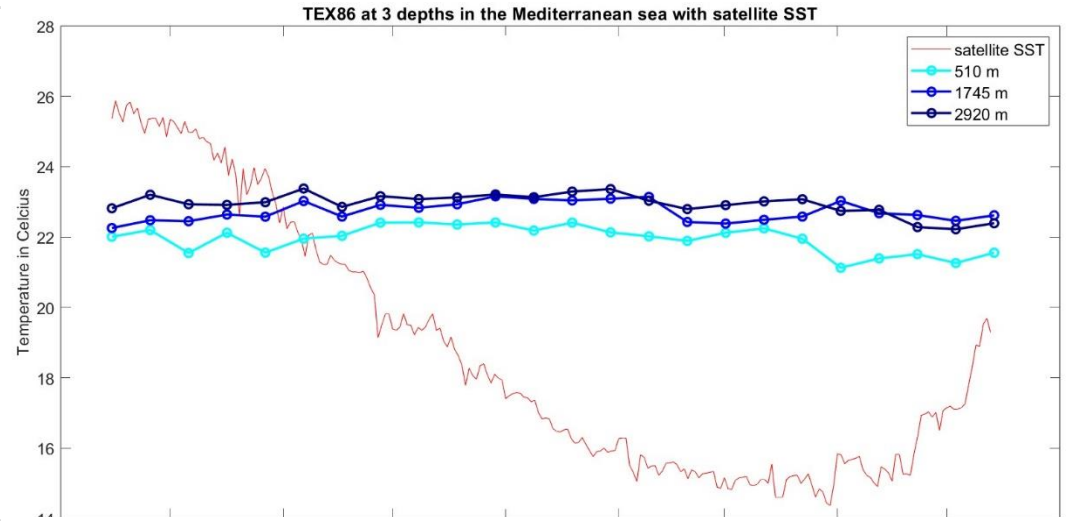


b.

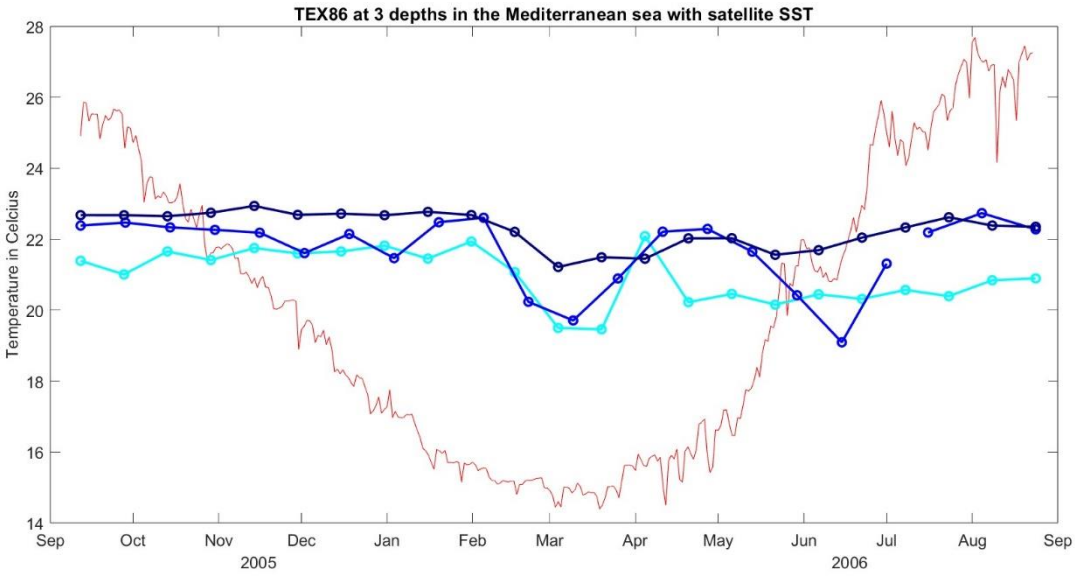


Fig. 5: SST estimates (using Eq. 4) derived from $TEX_{86}$ (using Eq. 3) from 3 sediment trap with satellite derived SST. (a.) from 15/09/1999 to 13/05/2000. (b.) from 12/09/2005 to 23/08/2006.

Table 5 shows the annual average $TEX_{86}$ predicted SST per sediment trap. For both years, sediment trap 3 predicts the highest temperatures. The difference between sediment trap 1 and sediment trap 3 predicted temperatures is largest from June through the summer of 2006, with an average difference of 1.7 ºC. During 1999/2000, $TEX_{86}$ predicted temperatures in sediment trap 1 are never higher than sediment trap 2 or 3. This sampling year also experiences a less variance in $TEX_{86}$ predicted temperatures than during 2005/2006. In 1999/2000 the $TEX_{86}$ ranges between 21.1 ºC and 23.4 ºC compared to a range between 19.1 ºC and 22.9 ºC during 2005/2006. All three sediment traps show a decrease in predicted temperature between the sampling years. On average, $TEX_{86}$ predicted temperature decreases by 0.9 ºC. The satellite derived SST increases between the sampling years with 1.3 ºC. Mainly caused by the missing summer months in the 2000 samples. On average, in 1999/2000, the $TEX_{86}$ signal overestimates SST with 3.9 ºC and in 2005/2006, with 1.6 ºC.

Table 5. Comparing satellite temperature measurements for both years and individual $TEX_{86}$ sediment trap measurements.

| | Satellite SST | Trap 1: 510 m | Trap 2: 1745 m | Trap 3: 2920 m |
|---|---|---|---|---|
| 1999/2000 | 18.7 ºC | 22.0 ºC | 22.7 ºC | 23.0 ºC |
| 2005/2006 | 20.0 ºC | 21.0 ºC | 21.7 ºC | 22.3 ºC |

During 1999/2000, sediment trap 3 has highest GDGT-2/GDGT-3 ratio with 13.4 on average. Sediment trap 2 has an average GDGT-2/GDGT-3 ratio of 12.0. Every sample of sediment trap 1 has a lower GDGT-2/GDGT-3 ratio than the other two sediment traps, being 9.1 on average (Fig. 6). From February, the GDGT-2/GDGT-3 ratio decreases for all three sediment traps, being … before February and … after February. In 2005/2006, the GDGT-2/GDGT-3 is highest for sediment trap 2 being 11.5 on average. Sediment trap 3 is 11.2 on average and sediment trap 1 has an average value of 8.7. Sediment trap 2 and 3 overlap each other on several occasions throughout the year. In February 2005/2006 the GDGT-2/GDGT-3 ratio goes from 12.5 to 6.2 on average across all three sediment traps. It remains relatively low in March and increases gradually from April onwards.

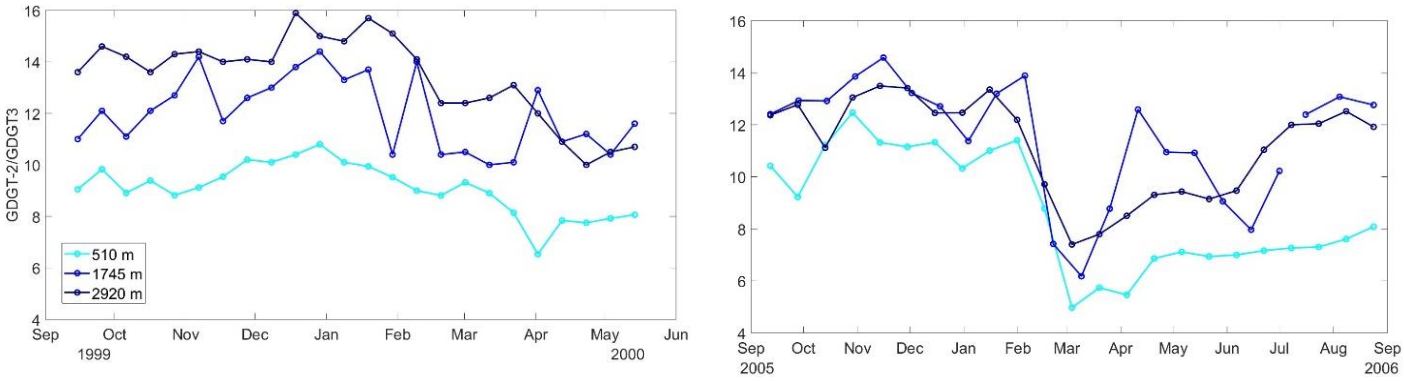


Fig. 6: GDGT-2/GDGT-3 ratio of both years for each sediment trap.

The ratio of GDGTs changes between sediment traps. Across sediment trap depths the relative influence of different version of GDGTs varies. GDGT-0 and GDGT-2 increase in relative influence on the $TEX_{86}$ calibration with depth and crenarchaeol shows the largest increase across the three sediment traps. The sediment traps show that the relative abundance of GDGT-1, GDGT-3 and cren' decreases with depth. The difference in GDGT ratio is larger between sediment trap 1 and 2 compared to the difference between sediment trap 2 and 3.

### *Other environmental parameters*

NPP is plotted for both years at 8 different depths in the Urania Basin using data acquired from the Global Ocean Biogeochemistry Hindcast (Fig A.1). It shows that autumn is characterised by relatively low values of 1 g $C/m^2$/day during both years. In January 2000 the NPP increases gradually in all measured depths except for 147 m and 200 m. It reaches maximum values of 5 g $C/m^2$/day in all surface layers in March. Sub-mixed layers of 78 m and 97 m depth show a maximum NPP of 4 g $C/m^2$/day in April and May, respectively. In 2005/2006, NPP increases in a more abrupt manner compared to 1999/2000 and later, namely, in February. In March all measured layers, except for 200 m depth, reach a NPP of 5 g $C/m^2$/day. Sub-mixed layers of 78 m and 97 m depth show a maximum NPP higher than 5 g $C/m^2$/day in late April and June, respectively.

Chlorophyl concentrations, obtained from the Global Ocean Biogeochemistry Hindcast, measured at different depths during 2005/2006 are plotted (Fig. A.2). This graph shows that the concentrations switch from being high at all plotted depths in March to being low at the surface and highest at 77 m depth in May.

The nitracline is calculated based on the nitrate change in concentration per meter (Fig. A.3). The nitracline is at 140 m depth during late autumn and early winter for both years. In March it switches to 160 m depth for 1999/2000 and to 170 m depth for 2005/2006.

Annual phosphorus concentration is depicted for 4 surface layer depths for both years (Fig. A.4). Phosphorus concentrations at each measured depth increase in November and reach a maximum concentrations at the end of February. Subsequently the phosphorus concentration decreases to practically 0 µmol/L in May where it stays throughout spring.

# Discussion

## Flux trends

The last sample measured in both years shows an extremely high biomarker flux. This high flux is not caused by an environmental factor. It is rather caused by the sediment trap being open during recovery, collecting material on its way up to the surface. For this reason, these values are excluded from the results.

$$U^{k}_{37}$$

The results in this research show relatively high long-chain alkenone production rates through an increased particle flux in sediment trap 1 in late winter/early spring of 1999/2000 and throughout spring in 2005/2006 (Fig. 5). This coincides with NPP increasing in February and maximizing in March in the layers <100 m depth of the Urania Basin. Unlike GDGTs, long-chain alkenones can in fact sink by themselves without needing faecal packaging and are exported throughout the year (Richey & Tierney, 2016). However, smaller particles do remain in the water column longer compared to aggregates and the flux is likely dominated by more rapidly sinking aggregates and faecal pellets (Thomsen et al., 1998).

When the alkenone flux is relatively high in May 2006, the NPP in the shallower layers of the water column are 3 times lower than those layers in March 2006. In May 2006 NPP is highest at 78 m water depth. This 78 m depth NPP peak could indicate a deepening of the depth distribution of Haptophyte algae after nutrients are depleted in shallower layers (Prahl et al., 1993; Ternois et al., 1996). It does not necessarily mean that Haptophyte algae migrate to exactly 78 m depth, as they still need enough sunlight to survive which is hard to achieve below 40 m depth (Cacho et al., 1999). Besides, NPP includes a lot more than just the production of Haptophyte algae; but this shift in NPP being higher in deeper layers does suggest a migration of micro-organisms to deeper waters. It also occurs when stratification starts to return in the Urania Basin and the exchange of nutrients between water layers decreases, causing nutrients to be depleted in near-surface layers (Leider et al., 2010). A few weeks before NPP in the surface layers decreases, phosphate in the same near-surface layers decreases.

The less high alkenone flux in spring of 2000 compared to spring 2006, can be explained by the less intense NPP values in spring 2000. NPP at 78 m depth in April 2000 reaches 4 g $C/m^2$/day and in April 2006 at the same depth NPP reaches 6 g $C/m^2$/day. A higher NPP increases the chances for alkenones to form aggregates, increasing the rate at which they are exported, increasing the alkenone flux.

The 78 m depth NPP peak in 1999/2000 is less separated from the shallow water depth peaks as in 2005/2006. It experiences a more gradual transition which could suggest there is less need for micro-organisms to rapidly migrate to deeper waters. This could be caused by a more gradual decrease in nutrient availability in surface waters and a slower initiation of stratification of the water column in the Urania Basin. This results in a less intense flux maximum in the spring of 2000. During summer, the thermocline in the Mediterranean increases, preventing transportation of nutrients between layers. A declining alkenone production in summer is likely caused by nutrient depletion in the euphotic zone (Ternois et al., 1996). Also, the more rapidly changing NPP in 2005/2006 could cause lower alkenone flux values in winter 2006 as NPP is low throughout January instead of gradually increasing in this month in 2000.

The flux weighted average shows the expected $U^k_{37}$ signal in surface sediment based on the annual flux of each sediment trap. The sediment traps lie relatively close to each other compared to the seasonal differences of the $U^k_{37}$ SST prediction. However, the sediment traps differ more compared to the flux weighted average of $TEX_{86}$. This suggests that the production and export depth of long-chain alkenones plays a more significant role in the proxy signal of surface sediments compared to the production and export depth of GDGTs. Across both years, the alkenone flux is highest from late winter to early spring. The flux weighted average of sediment trap 2 reflects the annual average $U^k_{37}$ best as it has got the least amount of alkenone flux variance annually. The expected surface sediment $U^k_{37}$ based on sediment trap 3 is closest to winter satellite SST. The $U^k_{37}$ is weighted towards winter temperatures as the maximum alkenone flux of sediment trap 3 is in late winter/early spring. The flux weighted average of sediment trap 1 predicts a $U^k_{37}$ surface sediment value closest to $U^k_{37}$ measurements of summer. The alkenone flux trend of sediment trap 1 causes the measurements to be weighted towards summer SST, which is when $U^k_{37}$ underestimates SST. This could be a cause for the annual underestimation offset found in surface sediment studies the Mediterranean.

Why the alkenone flux maximum of sediment trap 3 in March 2006 is not detected in sediment trap 2, is unclear. Long-chain alkenones reaching sediment trap 3 from elsewhere through for instance lateral transport or upwelling of particles is both unlikely. Lateral transport is an unlikely factor as SST at surface sediment and SST of the particles origine has a <0.2 ºC offset (Rice, et al., 2022). Upwelling is unlikely as there is >500 m between the depth of sediment trap 3 and the sea floor (Tanhua, et al., 2013).

Richey & Tierney (2016) do not find a consistent seasonal trend in the alkenone flux. Even if similarities between both sampled years in this research are visible, i.e. increased flux in March, a consistent seasonal pattern is not apparent. They also find a maximum winter flux which is paired with an organic carbon flux and primary productivity maximum at the same time. The results from this research find a maximum flux slightly later in February and May. Agreeing with Richey & Tierney (2016), a coinciding NPP maximum and alkenone flux maximum is found, supporting the idea that alkenone production is in line with NPP in the Urania Basin. Brassell (1993) did find a spring maximum alkenone flux, stating it is linked to a spring bloom of phytoplankton production. Sediment trap data from Nodder & Northcote (2001) in New Zealand shows spring/summer maximum flux of alkenones and particulate organic carbon being much higher than winter production. This proves that the seasonal

pattern of long-chain alkenone flux to the underlying sediment depends greatly on the location and year of sampling. Local NPP production trends can partly reveal the seasonal long-chain alkenone flux of a specific area.

Ternois et al. (1996) finds bi-seasonal export events in the alkenone flux with maximum production in October and a smaller but longer peak from April through May coinciding with the spring bloom period. A bi-seasonal export event is clearly visible in 2005/2006 with high values in early autumn and early spring. However, looking at both years, a maximum flux is found for the colder seasons of the year, February and March. An increased alkenone flux during the colder seasons is found to be characteristic for low-latitude locations (Bijma et al., 2001; Schneider et al., 2010). Schneider et al. (2010) further state that the varying alkenone flux could potentially induce a seasonal bias of annual $U^{k}_{37}$.

### *$TEX_{86}$*

In 1999/2000, the GDGT flux increases in winter and decreases halfway through spring. In 2005/2006, the GDGT flux increases at least a month later during late winter and decreases in summer. Both years also show one relatively higher flux sample point in December and January, respectively. Because GDGTs need methods like faecal packaging to sink, it is possible that GDGTs remain at the same depth in the water column for some time and only sink when NPP is high enough. This could potentially cause the $TEX_{86}$ signal to show temperatures at a delayed date and decrease the accuracy of SST predictions. The received signal in the sediment trap could potentially be a combination of signals from several dates as GDGTs do not immediately sink.

NPP in 1999/2000 increases in January and in 2005/2006 it increases later in February, coinciding with the delayed GDGT flux. When comparing the flux with annual NPP trends, a relation is found. These results show that a high NPP results in a higher GDGT flux. As NPP shows seasonality, so does the GDGT flux. However, this does not mean that the $TEX_{86}$ signal shows similar seasonality. The flux of Thaumarchaeota shows seasonality when the $TEX_{86}$ signal does not. A high or low GDGT flux does not lead to more variation in the $TEX_{86}$ signal or to a higher or lower sensitivity to SST change. During maximum flux in March 2000 and May 2006, measured in sediment trap 1, the $TEX_{86}$ signal does not show more variation or any sign of seasonality compared to the rest of the year. These results show that a higher GDGT flux does not cause more accurate $TEX_{86}$ SST predictions. The export of GDGTs does not predominantly take place when $TEX_{86}$ best predicts SST caused by the lack of variation and small range in the annual $TEX_{86}$ signal.

In February and March 2006, the $TEX_{86}$ signal does show variation in all sediment traps. February 2006 is the when the GDGT flux starts to increase, initially in sediment trap 3 followed by sediment trap 1. However, in spring, when the $TEX_{86}$ signal returns to a similar trends as before February, the flux in sediment trap 1 continues to increase. This makes it unlikely that the increase in flux in February caused the variation in the $TEX_{86}$ signal. There must be another driver that caused this variation.

The flux weighted average results show that each sediment trap has similar values. More similar than the flux weighted average of $U^{k}_{37}$. Suggesting that even though the flux of sediment trap 1 is higher than sediment trap 2 and 3 throughout the year, it has little effect on the $TEX_{86}$ predicted SST found in the underlying surface sediment. The similarity between the flux weighted averages suggests the $TEX_{86}$ results are not weighted towards a certain season despite the seasonality found in the GDGT flux. The predicted SST based on the flux weighted average shows a similar trend as the $TEX_{86}$ signal. Just like the $TEX_{86}$

signal, the flux weighted average of sediment trap 1 is lowest and that of sediment trap 3 is highest.

Considering the GDGT flux, Baxter et al. (2021) found great variety in the flux which was often highest in later winter/early spring, however, not consistent enough to be caused by annual cycles of water column mixing and stratification. Comparing the GDGT fluxes of each year from this research with each other, there are also clear differences noticeable. 1999/2000 is relatively higher in autumn and 2005/2006 seems a month behind the trends of the first year. However, just like Baxter et al. (2021) find, the GDGT flux is highest in late winter/early spring. Baxter et al. (2021), finds more annual variety in the $TEX_{86}$ signal than is found in this study. This is likely caused by the study location being a 90 m deep lake. Park, et al. (2018) found a similar winter increase of GDGT flux in the Atlantic Ocean compared to this research's results. However, they find relatively lower values in spring compared to the flux trends from this research.

The maximum abundance of Thaumarchaeota is between 140m and 170 m depth according to the depth of the nitracline. This depth is in line with the findings of Besseling et al. (2019). They suggest that Thaumarchaeota have a specific niche for sub-surface waters between 100 and 300 m depth. This is deeper compared to the Atlantic where the maximum abundance of Thaumarchaeota is located at 100 m depth (Herndl et al., 2005).

## Temperature predictions

### $U^k_{37}$

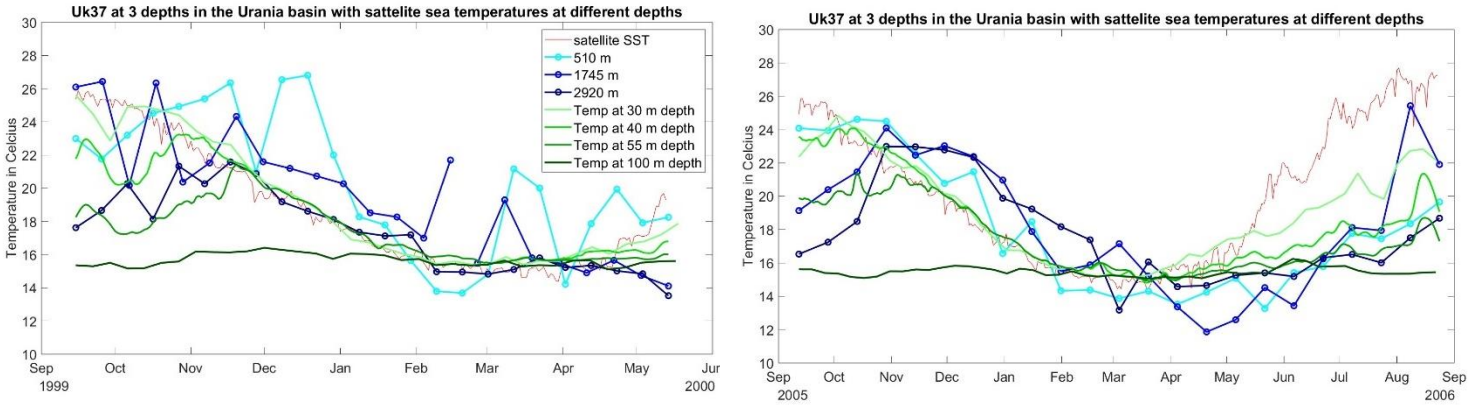


Fig. 7: $U^k_{37}$ signal of each sediment trap compared to measured temperatures at 5 depths in the water column.

The results of the temperature predictions given by $U^k_{37}$ show a clear seasonality. Both years predict the highest temperature when the satellite derived SST is highest, and the lowest temperatures are predicted when SST is the lowest. In autumn of 1999, the $U^k_{37}$ signal shows greater variance and individual sediment trap signals differ more from each other than later in the year. At this time of the year, the Mediterranean is most stratified (Malinverno et al., 2009). This stratification causes the already oligotrophic Mediterranean to be even more depleted of nutrients (Civitarese et al., 2010). Lower nutrient concentrations can cause Haptophyte algae to be more sensitive to temperature changes, possibly causing greater

variance in the $U^{k}_{37}$ signal (Conte et al., 2006). A larger variance in September and October is also measured in 2005. However, here it is less chaotic as sediment trap 1 gives a consistently higher temperature signal than the other two sediment traps. At times, there is a lag between the sediment trap 1 and sediment trap 2 and 3. This lag is not consistent. In December 1999 and August 2006, sediment trap 1 even seems to lag sediment trap 2 and 3. For most of the year, all three sediment traps have similar $U^{k}_{37}$ signals suggesting the long-chain alkenones in each sediment trap originate from a similar water depth. There is, however, a lag between each sediment trap and satellite SST, of one month on average. This lag is less in winter and increases in summer. The lag between satellite temperatures and the $U^{k}_{37}$ signals could be related to NPP. The transportation rate of particles already increases with wate depth, however, increased NPP accelerates this transportation rate (Miettinen et al., 2024). NPP is highest in March when the $U^{K}_{37}$ signal correlates with both SST and sub-mixed layer temperatures. Average NPP in the water column in November and December 2005 is lower than May and June 2006. With this in mind, a higher transportation rate of long-chain alkenones to the sediment traps is expected in the May-June paired with a shorter lag between the satellite temperatures and the $U^{k}_{37}$ signal at this time. However, the lag between SST and the $U^{k}_{37}$ signal is larger in May-June than November-December. This lag raises doubt if $U^{k}_{37}$ represents SST or rather sub-mixed layer temperatures. The satellite temperatures at 30 m, 40 m and 55 m depth are closer to the $U^{k}_{37}$ signal than SST (Fig. 7). The lag between the sediment trap signals and these sub-mixed layer temperatures even decreases in May-June, which is in line with the NPP trend. From May onward through spring and parts of summer, the depth at which long-chain alkenones are produced and exported from is possibly somewhere between those 30 m and 55 m depth. As Haptophyte algae live, predominantly, between 10 m and 40 m water depth in the Mediterranean (Cacho et al., 1999)., the production depth in spring and summer is likely below 30 m and not much more than 40 m. It is possible that the production depth of long-chain alkenones in autumn and winter is shallower. Vertical mixing peaks in winter in the Mediterranean, keeping surface layers fertilized with nutrients from deeper layers (Civitarese et al., 2010). Spring is characterised by the onset of stratification which increases throughout summer, preventing an input of nutrients to the surface layers of the Mediterranean (Civitarese et al., 2010). The subsequent depletion of nutrients in surface layers could cause Haptophyte algae to migrate to sub-mixed layers. The $U^{k}_{37}$ signal, therefore, correlates better with sub-mixed layer depth then SST in spring and summer.

When mixing is deepest in the winter months, the $U^{k}_{37}$ signal corresponds well to SST. However, during these months, temperature in sub-mixed layers is extremely similar SST due to the mixing of the water column in the Mediterranean. Therefore, annually, the $U^{k}_{37}$ signal represents sub-mixed layer temperatures of 40 m water depth best in the Urania Basin of the Mediterranean Sea. Tierney & Tingley (2018) propose the BAYSPLINE calibration model to predict $U^{k}_{37}$ temperatures. They state that BAYSPLINE prevents $U^{k}_{37}$ underestimating satellite SST. The results of this report show that an annual average underestimation of SST is not caused by the use of a linear calibration, rather by the fact the $U^{k}_{37}$ predicts sub-mixed layer temperatures instead of SST due to long-chain alkenones being produced in deeper layers.

Tierney & Tingley (2018) found the highest correlation between $U^{k'}_{37}$ and SST in the Mediterranean from January through April. This is accurate for the results in this report. The lowest correlations are from July through September, also agreeing with the results in this report. This is likely because during the months of January, February, March and April, the temperature at 30 m, 40 m and 55 m depth is extremely similar to SST due to extensive water column mixing.

*$TEX_{86}$*

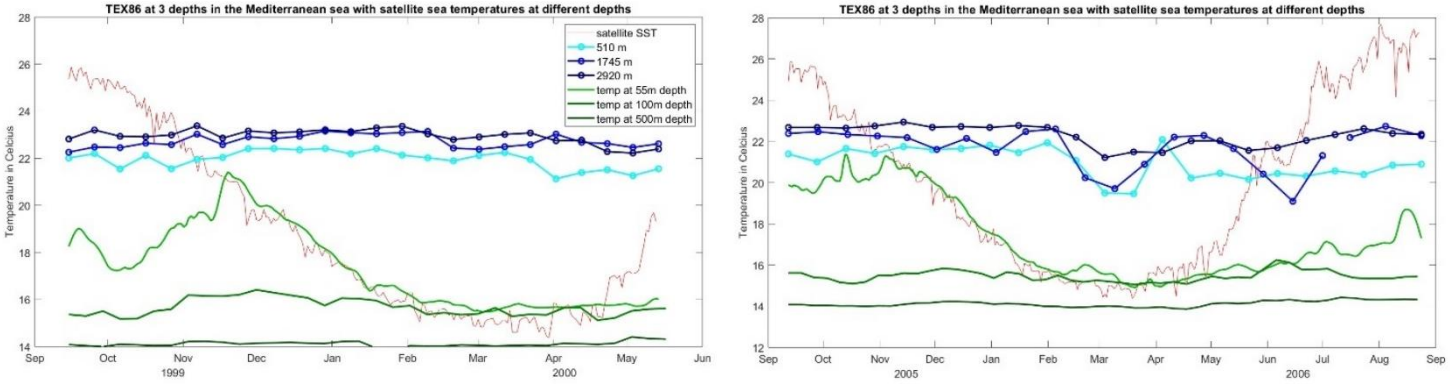


Fig. 8: $TEX_{86}$ signal of each sediment trap compared to measured temperatures at 5 depths in the water column.

The $TEX_{86}$ predicted temperature from the deepest sediment trap at, 2920 m depth, is consistently higher than the temperature signal coming from the shallowest sediment trap, at 510 m depth, except for one data point in April 2006 (Fig. 8). This goes against predictions that the deeper sediment trap would predict lower temperatures. Individual $TEX_{86}$ signals of each sediment trap only differ 1 ºC on average, suggesting the export depth of GDGTs does not differ much between sediment traps. Even when the nitracline shifts from 140 m in January 2000 to 160 m in March 2000, it does not influence the export depth of GDGTs enough to show variation in the $TEX_{86}$ signal. In 2005/2006, the shift of the nitracline from 140 m to 170 m depth in February happens at the same time as the decreased $TEX_{86}$ predicted SST. However, this is not proof that a deepening nitracline is a direct cause for decreased $TEX_{86}$ SST signal. Namely, apart from this correspondence, no clear relationship between the nitracline trend and the $TEX_{86}$ signal is found. This is likely because of the lack of seasonality of the proxy signal. It is expected that another environmental factor is responsible for the lack of seasonality of the $TEX_{86}$ signal.

Why sediment trap 3 is predicting the highest temperatures using $TEX_{86}$ can possibly be explained by the influence deep-dwelling Thaumarchaeota have on the $TEX_{86}$ signal in the Urania Basin. The GDGT-2/GDGT- 3 ratio results show that with increasing depth of the sediment trap, there is a increased chance of deep-dwelling Thaumarchaeota dominating the $TEX_{86}$ temperature signal (Fig. 6). The decrease in GDGT-2/GDGT-3 ratio in February and March 2006, suggests an increase in the fraction of surface Thaumarchaeal populations, is paired with decreased temperature predictions in all three sediment traps. February/March 2006 is the only time during both years that some form of seasonality is visible in the proxy signal. This suggests the $TEX_{86}$ signal shows more seasonal variation as the chance of surface Thaumarchaeota dominating the signal increases. An increased influence of surface Thaumarchaeota also results in lower $TEX_{86}$ temperature predictions. Perhaps, surface populations of Thaumarchaeota are more sensitive to SST variation compared to deep-dwelling Thaumarchaeota. Sediment trap 3 predicts the highest $TEX_{86}$ SST across both years and shows the highest average GDGT-2/GDGT-3 ratio in 1999/2000, being only slightly lower than sediment trap 2 in 2005/2006. It is likely that deep-dwelling Thaumarchaeota hold a different relation to growth temperature compared to surface populations of Thaumarchaeota. This is depicted in the results of this research by an increase in the degree of influence of deep-dwelling Thaumarchaeota resulting in increased $TEX_{86}$ SST prediction in the Mediterranean. Deep-dwelling Thaumarcheotal populations

likely play an important role in the overestimation of the $TEX_{86}$ SST prediction. The relation between deep-dwelling Thaumarchaeota and growth temperature is not yet fully understood. Their influence on $TEX_{86}$ is not widely researched yet. Villanueva et al., 2014 discovered they have distinct biosynthetic genes, however, the effect of which is a topic for future research. The results of this research suggest that they effect the $TEX_{86}$ paleotemperature proxy by causing an overestimation of SST.

This is not the only way deep-dwelling Thaumarchaeota could be influencing $TEX_{86}$ SST predictions. In March 2006, sediment trap 3 shows the lowest increased relative influence of surface Thaumarchaeota populations compared to the other two sediment traps. Sediment trap 3 also shows the smallest variation in $TEX_{86}$ SST prediction in March 2006. The largest relative change in the GDGT-2/GDGT-3 ratio in March 2006 is found in sediment trap 2, the same sediment trap that shows the biggest variation in its $TEX_{86}$ SST prediction. Deep-dwelling Thaumarchaeota influence could also play a significant role in the absent seasonality demonstrated by $TEX_{86}$ in this research.

Ionescu, et al. (2009), mentions that pelagic Thaumarchaeota assemblages in the Red Sea are phylogenetically distinct from populations living in close proximity to coral. The Arctic and Antarctic oceans also contain Thaumarchaeota distinct for each location with deep populations varying more than surface populations (Bano et al., 2004). There is no reason to think that in the Mediterranean, a deep-dwelling Thaumarchaeal population holds the same relation to temperature than surface populations (Besseling et al., 2019). Besides, surface- and deep Thaumarchaeota populations have distinct GDGT biosynthetic genes (Villanueva et al., 2014). According to Elling et al. (2014), Deep-dwelling populations are possibly adjusted to different nutrient concentrations compared to seasonal concentrations of surface waters of the Mediterranean adjusting their GDGT distributions. The $TEX_{86}$ signal of the individual sediment traps is line with Kim et al. (2015), who also found that the deep Mediterranean Thaumarchaeota community produces warmer $TEX_{86}$-derived SST compared to surface populations.

The difference between the GDGT-2/GDGT-3 ratio of sediment trap 2 and 3 is smaller than that between sediment trap 1 and 2. The same goes for the $TEX_{86}$ SST. Similar results are found in the Western Pacific Ocean by Guo, et al. (2024), where the GDGT-2/GDGT-3 values between 1000 m depth and 2000 m depth lie closer to each other than the ratio values between 500 m depth and 1000 m depth.

$TEX_{86}$ in the Eastern Mediterranean has been suggested to be skewed toward summer SST for off-shore sites, which is when the Mediterranean is most oligotrophic (Castañeda et al., 2010; Leider et al., 2010). The Urania Basin can be considered an off-shore site as terrestrial input is low. However, the $TEX_{86}$ signal from this report is not skewed toward summer SST. In fact, it is not skewed toward any season because of the lack of seasonality. According to Leider et al. (2010), an underestimation could be caused by non-oligotrophic conditions. The results from this research show an annual overestimation of SST by $TEX_{86}$. Which is in accordance with the year-round oligotrophic conditions found in the Mediterranean (Civitarese et al., 2010).

The annual $TEX_{86}$ overestimation of SST found in this report is also reported for off-shore sites in the Eastern Mediterranean by Leider et al. (2010). The limited amount of variation in the $TEX_{86}$ signal is similar to that of subsurface temperatures at 100 m and 500 m water depth. The $TEX_{86}$ signal greatly overestimates the sub-surface temperature because the $TEX_{86}$ signal is calibrated to SST instead of sub-surface temperature (Kim et al., 2015). The trend of the proxy signal showing little to no seasonality is in accordance with sub-surface temperatures. Huguet et al. (2011), state that the migration of Thaumarchaeota to deeper, colder water is unlikely to explain the overestimation of SST and sub-surface temperatures

in the Mediterranean. However, the increased influence of deep-dwelling Thaumarchaeota is not considered by Huguet et al. (2011) as a cause for the overestimation.

The lack of variation in in the $TEX_{86}$ signal causes it to not represent the seasonal pattern of the upper mixed layer temperature in the Urania Basin. Previous studies using modern samples from several locations, including the Mediterranean, concluded that $TEX_{86}$ better reflects sub-mixed layer temperatures between 30-200 m water depth (Lee et al., 2008; Jia et al., 2012; Kim et al., 2015). The $TEX_{86}$ results of this research agree better with the temperature trends at 100 m depth compared to the SST (Fig. 8).

## How do the proxy signals compare to SST?

### $U^k_{37}$

$U^k_{37}$ underestimates SST in 2005/2006 with 2 ºC. This is in accordance with previous research (Tierney & Tingley, 2018). This underestimation is not found in the sampling year of 1999/2000. Likely because this year is missing data points during spring and summer. This is when, during 2005/2006, the $U^k_{37}$ signal underestimates SST the most. This spring/summer underestimation is causing the annual underestimation of $U^k_{37}$ found in surface sediment studies (Ternois, 1996; Tierney & Tingley, 2018). The $U^k_{37}$ signal of the upper two sediment traps agree best with temperatures at 40 m water depth. The signal of sediment trap 3 agrees best with temperatures at 55 m water depth annually. From autumn until early spring, $U^k_{37}$ signal agrees with sub-mixed layer temperatures and SST equally as vertical mixing is causing these temperatures to be extremely similar.

Vertical mixing causes the $U^k_{37}$ signal to have little over- or underestimation in all 3 sediment traps during autumn, winter and early spring. Later in spring and throughout summer, the $U^k_{37}$ signal underestimates SST. During these months, until October, the $U^k_{37}$ better depicts sub-mixed layer temperatures at 40 m depth. This is likely caused by the stratification of the water column in the Urania Basin causing a depletion of nutrients in the surface layers (Civitarese et al., 2010). This forces Haptophyte algae to live in sub-mixed layer waters where they can find enough nutrients and still having enough sunlight to survive. There is a possibility that $U^k_{37}$ can live deeper than 40 m in during times of stratification in the Urania Basin. The Chlorophyl concentration deepens from March to May allowing sunlight to travel further through the water column. This could allow for Haptophyte algae to survive in deeper waters than 40 m (Cacho et al., 1999). This could explain why the $U^k_{37}$ signal of sediment trap 3 correlates best with water column temperature at 55 m instead of 40 m. Annually, $U^k_{37}$ better predicts SST than $TEX_{86}$ . However, $U^k_{37}$ better predicts sub-mixed layer temperature than SST.

Tierney & Tingley (2018) find a decreased correlation between SST and $U^k_{37}$ signal in summer in the Mediterranean. They find the highest correlation from January through April which is in agreement with the results of this research. However, they further state that the Mediterranean offset is due to a winter alkenone production bias. The flux weighted average could help to find out why this research does not agree with this statement. The flux weighted average of the $U^k_{37}$ sediment traps underestimates annual SST and is closest to satellite SST measured in spring. The flux weighted average of sediment trap 1 is closest to $U^k_{37}$ summer measurements which is when the $U^k_{37}$ signal underestimates satellite SST most. The flux weighted average of sediment trap 2 and 3 is closest to $U^k_{37}$ during winter and spring, when it depicts satellite SST accurately or with a smaller underestimation compared to summer. However, sediment trap 1 has the largest long-chain alkenone flux and its flux

weighted average, therefore, weighs the most. This suggests that $U^k_{37}$ paleotemperature records sampled from surface sediments or sediment cores are underestimating SST because of a late spring/early summer bias in the Urania Basin.

Future paleotemperature research should be aware of the underestimation during spring and summer. Especially in areas with strong seasonality related to a stratified water column, it could influence longer time scale $U^k_{37}$ records by underestimating SST predictions.

### *$TEX_{86}$*

$TEX_{86}$ lacks seasonality in its temperature prediction. On average, there is an overestimation of SST which becomes larger with a greater influence of deep-dwelling Thaumarchaeota, in accordance with Kim et al. (2015). However, a lack of seasonality is not always found in previous research. Variation in $TEX_{86}$ predictions is found in research across longer time scales in the Western-Mediterranean. Morcillo-Montalba et al. (2021) find a correlation between $TEX_{86}$ and $U^k_{37}$ for the past 35 kyr, with both proxies showing similar temperature ranges. The time scale does not even have to exceed several thousand years to find variation in the $TEX_{86}$ signal. Nieto-Moreno et al., 2013 measuring $TEX_{86}$ and $U^k_{37}$ during the last 2 millennia find the highest $TEX_{86}$ values during the Medieval Climate Anomaly and the lowest during the Little Ice Age. This suggests the $TEX_{86}$ lack of variation is limited to an annual or decadal scale and likely related to a consistent production bias through the influence of deep-sea Thaumarchaeota. The danger is that this production bias, even if only clearly visible on an annual scale, potentially has effect on the longer timescale $TEX_{86}$ SST predictions. This production bias can cause an overestimation of SST in the Mediterranean. Nieto-Moreno et al., 2013, find $TEX_{86}$ predicted SST 4-5 ºC higher than $U^k_{37}$ predicted SST. This is even higher than the average 3 ºC overestimation found in this research. They suggest $TEX_{86}$ signal represents summer temperatures as this is when Thaumarchaeota thrive in surface waters. This might be relevant for the Western Mediterranean. However, the results from this research show that in the Urania Basin, the largest influence of surface Thaumarchaeota is in March rather than in the summer. Besides, these results show that $TEX_{86}$ is not weighted toward a specific season as long as deep-sea Thaumarchaeota have a greater influence on the temperature signal than surface populations. Here, the extent of deep-sea Thaumarchaeota influence dictates the amount the $TEX_{86}$ signal overestimates annual SST.

However, the Western Mediterranean and elsewhere, might show different results and perhaps be weighted towards a specific season. The Western Mediterranean is less deep than the Urania Basin and, therefore, the influence of deep-sea Thaumarchaeota might be less dominant. This could cause the seasonal production of GDGTs to influence the $TEX_{86}$ signal (Nieto-Moreno et al., 2013). In the Urania Basin, $TEX_{86}$ does not represent SST better during one season than another because more GDGTs are exported during that season. Here, the $TEX_{86}$ signal happens to represent a specific time of the year based on the degree of overestimation by $TEX_{86}$. The predicted overestimation is decided by the degree of deep-dwelling Thaumarchaeota influence.

According to Huguet et al. (2011), in the Western Mediterranean, $TEX_{86}$ derived temperatures generally agree with or are higher than $U^k_{37}$ derived temperatures. The sediment trap measurement from this research show that $TEX_{86}$ temperatures are higher on average than $U^k_{37}$, even though Thaumarchaeota live in deeper waters than Haptophyte algae. Thaumarchaeota, and specifically deep-dwelling populations, likely have a more complex relation to the growth temperature than Haptophyte algae do. The sensitivity of GDGTs to temperature depends more strongly on the depth Thaumarchaeota populations

produce GDGTs (Kim et al., 2015; Besseling et al., 2019). In paleoclimatology studies, proxies are often sampled from surface sediments. These proxy signals represent a multi-annual average temperature signal and are not season specific. The flux weighted average of $TEX_{86}$ predicts a surface sediment signal that overestimates annual SST by about 1 ºC.

## Ratios of GDGTs and long-chain alkenones with water depth

Sediment trap 1 shows a greater variability than sediment trap 2 and 3. It seems that the deeper the sediment trap, the more stable the $U^k_{37}$ signal is. Similar trends are visible with satellite temperature. Temperature at the surface varies greatly as it is more sensitive to short term variations in the atmosphere and sunlight. In deeper water layers, the influence of sunlight decreases as it takes longer for heat to be conducted to those layers. Similar trends are visible comparing each sediment trap. The deepest sediment trap shows the least amount of variety because trends of environmental factors like nutrient concentrations are combined with other factors like lateral transport and a transportation delay preventing them from showing more detail. This causes the proxy signal to be blended in with trends of surrounding days and weeks before they reach sediment trap 3. In sediment trap 1, weekly $U^k_{37}$ changes are visible, but as you go deeper the $U^k_{37}$ signal starts lacking short term trends and shows more gradual changes as the biomarker of the surrounding days are mixed with the proxy signal.

Besseling et al. (2019), measured the ratio of different forms of GDGTs through the water column. They found that the total concentration of GDGTs and difference in ratio's in suspended particulate matter decrease exponentially from 300 m water depth until 1500 m depth after which it remains relatively equal for all GDGTs. This is in line with the GDGT ratios differing more between sediment trap 1 and 2 than between sediment trap 2 and 3. The increasing abundance of GDGT-2 and decreasing abundance of GDGT-3 agrees with Guo et al. (2024). They also find a larger change in relative GDGT-2 and GDGT-3 influence from 500 m to 1000 m than from 1000m to 2000 m. Besseling et al. (2019) also find an increasing abundance of GDGT-0, GDGT-2 below 500 m depth in the Mediterranean. Besseling et al. (2019) find differing trends in more shallow depths <300 m. They find an increasing abundance of GDGT-1 and cren' up to 300 m depth. The most significant changes in GDGT ratios are in depths <300 m and they could change in deeper layers. GDGT-0 decreases with depth <500 m and increases >500 m. In deeper layers, abundance trends are less apparent concerning these GDGTs (Besseling et al., 2019). This results in the $TEX_{86}$ SST prediction of sediment trap 2 and 3 being more similar than sediment trap 1 in this research. The GDGT ratio changing between sediment traps could be the cause of a transportation bias. It seems that GDGT-1, GDGT-3 and cren' are less likely to reach sediment trap 2 and 3 compared to other GDGTs. However, it could also be caused by deep-dwelling Thaumarchaeota producing GDGT at different ratios compared to surface Thaumarchaeota, causing the trends to change >500 m depth.

## Environmental mechanisms driving export of biomarkers

As $U^k_{37}$ shows more seasonality, it is easier to notice similarities between nutrient concentrations and the proxy signal. When phosphate concentrations are high, so is the correlation of $U^k_{37}$ with satellite SST. At this time, late winter/early spring, NPP is highest in

surface layers. When NPP maximum values shift to sub-mixed layer depths, between 50 m and 100 m, the $U^k_{37}$ signal correlates best with sub-mixed layer depths at 40 m, suggesting a deepening of the formation depth of long-chain alkenones (Kim et al., 2015). This better accordance with sub-mixed layer temperatures continues through summer as stratification of the water column increases during summer in the Mediterranean (Malinverno et al., 2009; Civitarese et al., 2010). The results from this research find a negative correlation between NPP and SST. NPP increases when SST decreases in the Urania Basin, which Schneider et al. (2010) claims to be characteristic for low-latitude locations. The alkenone flux trend of this research shows that it follows this relation described by Scheider et al. (2010) apart from still showing a larger flux during spring. This is likely caused by NPP still being higher in sub-mixed layer depths in early spring. This, in turn, causes lower $U^k_{37}$ SST predictions because of the negative relation between NPP and SST. A better agreement of $U^k_{37}$ with SST when NPP is higher in surface layers is also found in Tierney and Tingley (2018). During autumn, stratification decreases and water column mixing increases, causing nutrients to gradually return to surface waters followed by Haptophyte algae. This causes the alkenone flux to increase in winter. However, flux maximises during the spring bloom in the Urania Basin right before nutrients like phosphate are depleted once again. Correlation between $U^k_{37}$ and SST is highest in winter agreeing with Ternois et al. (1996). This is when vertical mixing, driven mostly by wind stress, is high and surface nutrients are not yet depleted (Malinverno et al., 2009).

Tierney & Tingley (2014) describe the phenomenon of lower nutrient availability resulting in an increased sensitivity of $TEX_{86}$ SST predictions. This is not found in the results of this research. When the Urania Basin is most depleted of phosphorus and nitrate, the $TEX_{86}$ does not show more variability or any form of seasonality. The only time increased sensitivity of $TEX_{86}$ SST predictions is depicted is when nutrient availability is relatively high and vertical mixing is most intense in the Urania Basin. However, even this variation is minimal and cannot be seen as $TEX_{86}$ showing seasonality.

If nutrient concentrations in the Mediterranean were a large driver of the $TEX_{86}$ signal, the results from this research would have shown some form of seasonality. The lack of which suggests a different factor is dominating the influence on the signal. Thaumarchaeota are some of the main ammonia oxidisers in the water column in the Mediterranean. They have been proven to respond quickly to fluctuations in ammonia concentrations (Beman et al., 2012). This would cause variation in the production and export depth of GDGTs. Seasonal fluctuations in the nitrate concentrations with depth and of the nitracline are apparent in the Urania Basin (Global Ocean Biogeochemistry Hindcast; Fig. A.3). However, this does not seem to affect the $TEX_{86}$ signal enough to show any form of seasonality.

Nieto-Moreno et al., (2013) find a greater surface production of biomarkers in summer, which shows that even within the Mediterranean, results can differ as environmental mechanisms are extremely local. Therefore, research using sediment traps at different depths is needed in other locations to identify the consistency of trends found in this research.

It must be considered that no $TEX_{86}$ or $U^k_{37}$ signal is measured for the years in between 1999/2000 and 2005/2006. The years in between could reveal a different pattern than the results of this research. A multi-year monitoring proxy could potentially be extremely helpful to analyse seasonal trends of either proxy. in greater detail. Comparing the two years measured for this research, differences are already apparent. A multi-year monitoring proxy has the capability to follow the progress of both paleotemperature proxies in greater detail, allowing for a reliable future projection of SST in the Mediterranean.

# Conclusions

A seasonal pattern is clearly visible in the annual flux of long-chain alkenones and GDGTs. On average, the flux is highest when vertical mixing is at its maximum in the Urania Basin, in later winter/early spring. When the water column becomes more stratified, long-chain alkenone and GDGT flux decreases. This seasonality is visible in the $U^{k}_{37}$ SST prediction which is most accurate when vertical mixing is high. During spring and summer, $U^{k}_{37}$ underestimates SST and starts to represent sub-mixed layer temperatures better. This is caused by the depletion of nutrients in surface layers with the onset of stratification in the Urania Basin. Through long-chain alkenone flux, a late spring/early summer bias is found for $U^{k}_{37}$ causing an annual underestimation of SST.

A lack of seasonality is found for the $TEX_{86}$ SST prediction. This is caused by the influence of deep-dwelling Thaumarchaeota in the Mediterranean. They decrease the sensitivity of the $TEX_{86}$ signal to SST variation. They also likely hold a different relation to growth temperature causing an annual overestimation of SST. As long as deep-dwelling Thaumarchaeota hold great influence on the $TEX_{86}$ signal, it is unlikely that $TEX_{86}$ holds any bias towards a specific season.

$U^{k}_{37}$ holds a better agreement with SST than $TEX_{86}$ throughout the year. However, the predicted surface sediment signal of $U^{k}_{37}$ differs more between sediment traps than $TEX_{86}$ signal. This increases the likelihood for surface sediment studies to be biased towards a specific season. The individual sediment traps of $TEX_{86}$ are in better agreement making surface sediment studies less likely to be influenced by variations concerning biomarker production and export depths..

# References


Bano, N., Ruffin, S., Ransom, B., & Hollibaugh, J. T. (2004). Phylogenetic composition of Arctic Ocean archaeal assemblages and comparison with Antarctic assemblages. *Applied and Environmental Microbiology*, *70*(2), 781-789.

Beman, J. M., Popp, B. N., & Alford, S. E. (2012). Quantification of ammonia oxidation rates and ammonia-oxidizing archaea and bacteria at high resolution in the Gulf of California and eastern tropical North Pacific Ocean. *Limnology and Oceanography*, *57*(3), 711-726.

Besseling, M. A., Hopmans, E. C., Koenen, M., van der Meer, M. T., Vreugdenhil, S., Schouten, S., ... & Villanueva, L. (2019). Depth-related differences in archaeal populations impact the isoprenoid tetraether lipid composition of the Mediterranean Sea water column. *Organic Geochemistry*, *135*, 16-31.

Bijma, J., Altabet, M., Conte, M., Kinkel, H., Versteegh, G. J. M., Volkman, J. K., ... & Weaver, P. P. (2001). Primary signal: Ecological and environmental factors—Report from Working Group 2. *Geochemistry, Geophysics, Geosystems*, *2*(1).

Brassell, S. C., Brereton, R. G., Eglinton, G., Grimalt, J., Liebezeit, G., Marlowe, I. T., ... & Sarnthein, M. (1986). Palaeoclimatic signals recognized by chemometric treatment of molecular stratigraphic data. *Organic Geochemistry*, *10*(4-6), 649-660.

Brassell, S. C. (1993). Applications of biomarkers for delineating marine paleoclimatic fluctuations during the Pleistocene. In *Organic geochemistry: Principles and applications* (pp. 699-738). Boston, MA: Springer US.

van Boxtel, A., Rice, A., de Lange, G., Peterse, F., & Stuut, J. B. (2023, May). Assessing the relationship between Saharan dust input and export of organic material in the deep eastern Mediterranean Sea using a one-year sediment-trap record. In *EGU General Assembly Conference Abstracts* (pp. EGU-15181).

Cacho, I., Pelejero, C., Grimalt, J. O., Calafat, A., & Canals, M. (1999). C37 alkenone measurements of sea surface temperature in the Gulf of Lions (NW Mediterranean). *Organic Geochemistry*, *30*(7), 557-566.

Castañeda, I. S., Schefuß, E., Pätzold, J., Sinninghe Damsté, J. S., Weldeab, S., & Schouten, S. (2010). Millennial-scale sea surface temperature changes in the eastern Mediterranean (Nile River Delta region) over the last 27,000 years. *Paleoceanography*, *25*(1).

Civitarese, G., Gačić, M., Lipizer, M., & Eusebi Borzelli, G. L. (2010). On the impact of the Bimodal Oscillating System (BiOS) on the biogeochemistry and biology of the Adriatic and Ionian Seas (Eastern Mediterranean). *Biogeosciences*, *7*(12), 3987-3997.

Conte, M. H., Sicre, M. A., Rühlemann, C., Weber, J. C., Schulte, S., Schulz-Bull, D., & Blanz, T. (2006). Global temperature calibration of the alkenone unsaturation index (UK′ 37) in surface waters and comparison with surface sediments. *Geochemistry, Geophysics, Geosystems*, *7*(2).

Corselli, C., Principato, M. S., Maffioli, P., & Crudeli, D. (2002). Changes in planktonic assemblages during sapropel S5 deposition: Evidence from Urania Basin area, eastern Mediterranean. *Paleoceanography*, *17*(3), 1-1.

Damsté, J. S. S., Schouten, S., Hopmans, E. C., Van Duin, A. C., & Geenevasen, J. A. (2002). Crenarchaeol. *Journal of lipid research*, *43*(10), 1641-1651.

De Corte, D., Yokokawa, T., Varela, M. M., Agogué, H., & Herndl, G. J. (2009). Spatial distribution of Bacteria and Archaea and amo A gene copy numbers throughout the water column of the Eastern Mediterranean Sea. *The ISME journal*, *3*(2), 147-158.

Elling, F. J., Könneke, M., Lipp, J. S., Becker, K. W., Gagen, E. J., & Hinrichs, K. U. (2014). Effects of growth phase on the membrane lipid composition of the thaumarchaeon Nitrosopumilus maritimus

and their implications for archaeal lipid distributions in the marine environment. *Geochimica et Cosmochimica Acta*, *141*, 579-597.

Francis, C. A., Roberts, K. J., Beman, J. M., Santoro, A. E., & Oakley, B. B. (2005). Ubiquity and diversity of ammonia-oxidizing archaea in water columns and sediments of the ocean. *Proceedings of the National Academy of Sciences*, *102*(41), 14683-14688.

*Global Ocean Biogeochemistry Hindcast.* Copernicus Marine Service. https://data.marine.copernicus.eu/product/GLOBAL_MULTIYEAR_BGC_001_029/description

*Global Ocean Physics Reanalysis.* Copernicus Marine Service. https://data.marine.copernicus.eu/product/GLOBAL_MULTIYEAR_PHY_001_030/description

Guo, J., Wang, Z., Achterberg, E. P., Yuan, H., Song, J., Wang, Y., ... & Qu, B. (2024). Variations in isoprenoid tetraether lipids through the water column of the Western Pacific Ocean: Implications for sedimentary TEX86 records. *Geochimica et Cosmochimica Acta*, *368*, 24-33.

Hallam, S. J., Mincer, T. J., Schleper, C., Preston, C. M., Roberts, K., Richardson, P. M., & DeLong, E. F. (2006). Pathways of carbon assimilation and ammonia oxidation suggested by environmental genomic analyses of marine Crenarchaeota. *PLoS biology*, *4*(4), e95.

Hernández-Sánchez, M. T., Woodward, E. M. S., Taylor, K. W. R., Henderson, G. M., & Pancost, R. D. (2014). Variations in GDGT distributions through the water column in the South East Atlantic Ocean. *Geochimica et Cosmochimica Acta*, *132*, 337-348.

Ho, S. L., & Laepple, T. (2016). Flat meridional temperature gradient in the early Eocene in the subsurface rather than surface ocean, Nat. Geosci., 9, 606–610.

Herndl, G. J., Reinthaler, T., Teira, E., van Aken, H., Veth, C., Pernthaler, A., & Pernthaler, J. (2005). Contribution of Archaea to total prokaryotic production in the deep Atlantic Ocean. *Applied and environmental microbiology*, *71*(5), 2303-2309.

Huguet, C., Martrat, B., Grimalt, J. O., Sinninghe Damsté, J. S., & Schouten, S. (2011). Coherent millennial-scale patterns in U37k′ and TEX86H temperature records during the penultimate interglacial-to-glacial cycle in the western Mediterranean. *Paleoceanography*, *26*(2).

Ionescu, D., Penno, S., Haimovich, M., Rihtman, B., Goodwin, A., Schwartz, D., ... & Oren, A. (2009). Archaea in the Gulf of Aqaba. *FEMS microbiology ecology*, *69*(3), 425-438.

Iversen, M. H., & Ploug, H. (2010). Ballast minerals and the sinking carbon flux in the ocean: carbon-specific respiration rates and sinking velocity of marine snow aggregates. *Biogeosciences*, *7*(9), 2613-2624.

Jia, G., Zhang, J., Chen, J., Peng, P., & Zhang, C. L. (2012). Subsurface water temperatures recorded by archaeal tetraether lipids in the South China Sea. *Organic Geochemistry*, *50*, 68-77.

Kim, J. H., Van der Meer, J., Schouten, S., Helmke, P., Willmott, V., Sangiorgi, F., ... & Damsté, J. S. S. (2010). New indices and calibrations derived from the distribution of crenarchaeal isoprenoid tetraether lipids: Implications for past sea surface temperature reconstructions. *Geochimica et Cosmochimica Acta*, *74*(16), 4639-4654.

Kim, J. H., Schouten, S., Rodrigo-Gámiz, M., Rampen, S., Marino, G., Huguet, C., ... & Damsté, J. S. S. (2015). Influence of deep-water derived isoprenoid tetraether lipids on the TEX86H paleothermometer in the Mediterranean Sea. *Geochimica et Cosmochimica Acta*, *150*, 125-141.

Kim, J. H., Villanueva, L., Zell, C., & Damsté, J. S. S. (2016). Biological source and provenance of deep-water derived isoprenoid tetraether lipids along the Portuguese continental margin. *Geochimica et Cosmochimica Acta*, *172*, 177-204.

Krom, M. D., Brenner, S., Kress, N., Neori, A., & Gordon, L. I. (1992). Nutrient dynamics and new production in a warm-core eddy from the Eastern Mediterranean Sea. *Deep Sea Research Part A. Oceanographic Research Papers*, *39*(3-4), 467-480.

Lee, K. E., Kim, J. H., Wilke, I., Helmke, P., & Schouten, S. (2008). A study of the alkenone, TEX86, and planktonic foraminifera in the Benguela Upwelling System: Implications for past sea surface temperature estimates. *Geochemistry, Geophysics, Geosystems*, *9*(10).

Leider, A., Hinrichs, K. U., Mollenhauer, G., & Versteegh, G. J. (2010). Core-top calibration of the lipid-based U37K′ and TEX86 temperature proxies on the southern Italian shelf (SW Adriatic Sea, Gulf of Taranto). *Earth and Planetary Science Letters*, *300*(1-2), 112-124.

Malinverno, E., Triantaphyllou, M. V., Stavrakakis, S., Ziveri, P., & Lykousis, V. (2009). Seasonal and spatial variability of coccolithophore export production at the South-Western margin of Crete (Eastern Mediterranean). *Marine Micropaleontology*, *71*(3-4), 131-147.

Miettinen, T. P., Gomez, A. L., Wu, Y., Wu, W., Usherwood, T. R., Hwang, Y., ... & Manalis, S. R. (2024). Cell size, density, and nutrient dependency of unicellular algal gravitational sinking velocities. *Science Advances*, *10*(27), eadn8356.

Morcillo-Montalbá, L., Rodrigo-Gámiz, M., Martínez-Ruiz, F., Ortega-Huertas, M., Schouten, S., & Sinninghe Damsté, J. S. (2021). Rapid Climate Changes in the Westernmost Mediterranean (Alboran Sea) Over the Last 35 kyr: New Insights From Four Lipid Paleothermometers (UK'37, TEXH86, RI-OH', and LDI). *Paleoceanography and Paleoclimatology*, *36*(12), e2020PA004171.

Mollenhauer, G., Eglinton, T. I., Hopmans, E. C., & Damsté, J. S. S. (2008). A radiocarbon-based assessment of the preservation characteristics of crenarchaeol and alkenones from continental margin sediments. *Organic Geochemistry*, *39*(8), 1039-1045.

Mollenhauer, G., Basse, A., Kim, J. H., Damste, J. S. S., & Fischer, G. (2015). A four-year record of UK′ 37-and TEX86-derived sea surface temperature estimates from sinking particles in the filamentous upwelling region off Cape Blanc, Mauritania. *Deep Sea Research Part I: Oceanographic Research Papers*, *97*, 67-79.

Nicholls, K. H. (2015). Haptophyte algae. In *Freshwater Algae of North America* (pp. 587-605). Academic Press.

Nieto-Moreno, V., Martínez-Ruiz, F., Willmott, V., García-Orellana, J., Masqué, P., & Damsté, J. S. (2013). Climate conditions in the westernmost Mediterranean over the last two millennia: An integrated biomarker approach. *Organic Geochemistry*, *55*, 1-10.

Nodder, S. D., & Northcote, L. C. (2001). Episodic particulate fluxes at southern temperate mid-latitudes (42–45 S) in the Subtropical Front region, east of New Zealand. *Deep Sea Research Part I: Oceanographic Research Papers*, *48*(3), 833-864.

Polymenakou, P. N., Stephanou, E. G., Tselepides, A., & Bertilsson, S. (2007). Organic matter preservation and microbial community accumulations in deep-hypersaline anoxic Basins. *Geomicrobiology Journal*, *24*(1), 19-29.

Prahl, F. G., Muehlhausen, L. A., & Zahnle, D. L. (1988). Further evaluation of long-chain alkenones as indicators of paleoceanographic conditions. *Geochimica et Cosmochimica Acta*, *52*(9), 2303-2310.

Prahl, F. G., & Wakeham, S. G. (1987). Calibration of unsaturation patterns in long-chain ketone compositions for palaeotemperature assessment. *Nature*, *330*(6146), 367-369.

Prahl, F. G., Collier, R. B., Dymond, J., Lyle, M., & Sparrow, M. A. (1993). A biomarker perspective on prymnesiophyte productivity in the northeast Pacific Ocean. *Deep Sea Research Part I: Oceanographic Research Papers*, *40*(10), 2061-2076.

Prahl, F. G., Sparrow, M. A., & Wolfe, G. V. (2003). Physiological impacts on alkenone paleothermometry. *Paleoceanography*, *18*(2).

Rice, A., Nooteboom, P. D., Van Sebille, E., Peterse, F., Ziegler, M., & Sluijs, A. (2022). Limited lateral transport bias during export of sea surface temperature proxy carriers in the Mediterranean Sea. *Geophysical Research Letters*, *49*(4), e2021GL096859.

Richey, J. N., & Tierney, J. E. (2016). GDGT and alkenone flux in the northern Gulf of Mexico: Implications for the TEX86 and UK'37 paleothermometers. *Paleoceanography*, *31*(12), 1547-1561.

Rodrigo-Gámiz, M., Martínez-Ruiz, F., Rampen, S. W., Schouten, S., & Sinninghe Damsté, J. S. (2014). Sea surface temperature variations in the western Mediterranean Sea over the last 20 kyr: A dual-organic proxy (UK′ 37 and LDI) approach. *Paleoceanography*, *29*(2), 87-98.

Rosell-Melé, A., & Prahl, F. G. (2013). Seasonality of UK′ 37 temperature estimates as inferred from sediment trap data. *Quaternary Science Reviews*, *72*, 128-136.

Sass, A. M., Sass, H., Coolen, M. J., Cypionka, H., & Overmann, J. (2001). Microbial communities in the chemocline of a hypersaline deep-sea Basin (Urania Basin, Mediterranean Sea). *Applied and Environmental Microbiology*, *67*(12), 5392-5402.

Schneider, B., Leduc, G., & Park, W. (2010). Disentangling seasonal signals in Holocene climate trends by satellite-model-proxy integration. *Paleoceanography*, *25*(4).

Schouten, S., Hopmans, E. C., Schefuß, E., & Damste, J. S. S. (2002). Distributional variations in marine crenarchaeotal membrane lipids: a new tool for reconstructing ancient sea water temperatures?. *Earth and Planetary Science Letters*, *204*(1-2), 265-274.

Schouten, S., Forster, A., Panoto, F. E., & Damsté, J. S. S. (2007). Towards calibration of the TEX86 palaeothermometer for tropical sea surface temperatures in ancient greenhouse worlds. *Organic Geochemistry*, *38*(9), 1537-1546.

Schouten, S., Hopmans, E. C., & Damsté, J. S. S. (2013). The organic geochemistry of glycerol dialkyl glycerol tetraether lipids: A review. *Organic geochemistry*, *54*, 19-61.

Sollai, M. (2018). *Lipids as indicators of nitrogen cycling in present and past anoxic oceans* (Doctoral dissertation, UU Dept. of Earth Sciences).

Tanhua, T., Hainbucher, D., Schroeder, K., Cardin, V., Álvarez, M., & Civitarese, G. (2013). The Mediterranean Sea system: a review and an introduction to the special issue. *Ocean Science*, *9*(5), 789-803.

Taylor, K. W., Huber, M., Hollis, C. J., Hernandez-Sanchez, M. T., & Pancost, R. D. (2013). Re-evaluating modern and Palaeogene GDGT distributions: Implications for SST reconstructions. *Global and Planetary Change*, *108*, 158-174.

Ternois, Y., Sicre, M. A., Boireau, A., Marty, J. C., & Miquel, J. C. (1996). Production pattern of alkenones in the Mediterranean Sea. *Geophysical Research Letters*, *23*(22), 3171-3174.

Ternois, Y., Sicre, M. A., Boireau, A., & Conte, M. H. (1997). Evaluation of long-chain alkenones as paleo-temperature indicators in the Mediterranean Sea. *Deep Sea Research Part I: Oceanographic Research Papers*, *44*(2), 271-286.

Ternon, E., Guieu, C., Loÿe-Pilot, M. D., Leblond, N., Bosc, E., Gasser, B., ... & Martín, J. (2010). The impact of Saharan dust on the particulate export in the water column of the North Western Mediterranean Sea. *Biogeosciences*, *7*(3), 809-826.

Thomsen, C., Schulz-Bull, D. E., Petrick, G., & Duinker, J. C. (1998). Seasonal variability of the long-chain alkenone flux and the effect on the U37k′-index in the Norwegian Sea. *Organic Geochemistry*, *28*(5), 311-323.

Tierney, J. E., & Tingley, M. P. (2014). A Bayesian, spatially-varying calibration model for the TEX86 proxy. *Geochimica et Cosmochimica Acta*, *127*, 83-106.

Tierney, J. E., & Tingley, M. P. (2018). BAYSPLINE: A new calibration for the alkenone paleothermometer. *Paleoceanography and Paleoclimatology*, *33*(3), 281-301.

van der Weijst, C. M. H., van der Laan, K. J., Peterse, F., Reichart, G. J., Sangiorgi, F., Schouten, S., ... & Sluijs, A. (2022). A 15-million-year surface-and subsurface-integrated TEX86 temperature record from the eastern equatorial Atlantic, Clim. Past, 18, 1947–1962.

Villanueva, L., Schouten, S., & Sinninghe Damsté, J. S. (2015). Depth-related distribution of a key gene of the tetraether lipid biosynthetic pathway in marine T haumarchaeota. *Environmental microbiology*, *17*(10), 3527-3539.

Wuchter, C., Schouten, S., Wakeham, S. G., & Sinninghe Damsté, J. S. (2005). Temporal and spatial variation in tetraether membrane lipids of marine Crenarchaeota in particulate organic matter: Implications for TEX86 paleothermometry. *Paleoceanography*, *20*(3).

Ziveri, P., Rutten, A., De Lange, G. J., Thomson, J., & Corselli, C. (2000). Present-day coccolith fluxes recorded in central eastern Mediterranean sediment traps and surface sediments. *Palaeogeography, Palaeoclimatology, Palaeoecology*, *158*(3-4), 175-195.

# Appendix

a.

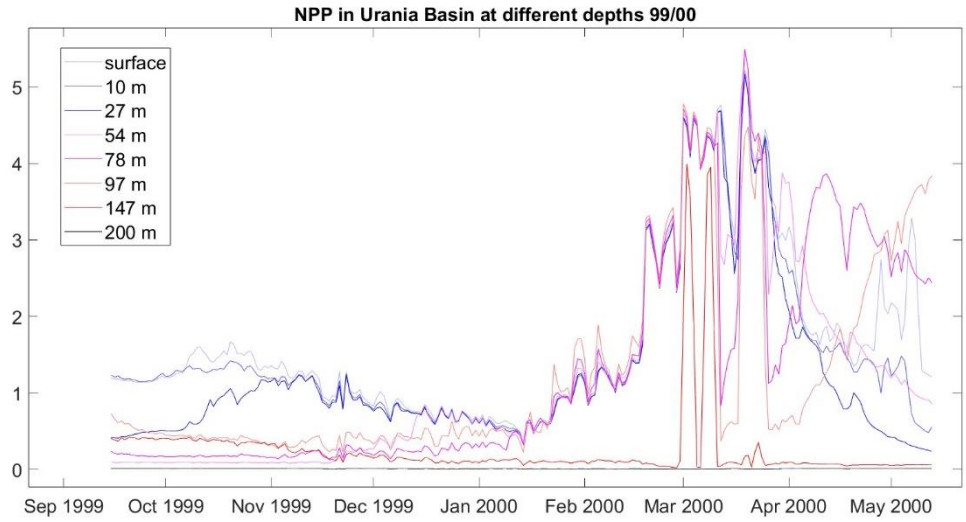


b.

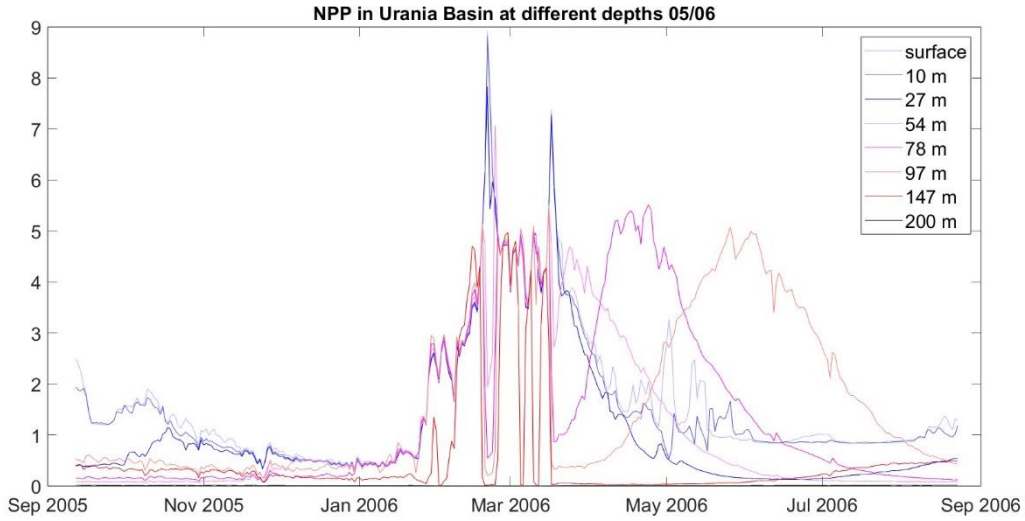


Fig A.1: a. Net Primary Production (NPP) in g C/$m^2$/day at eight depths in the water column in the Urania Basin during 1999/2000. b. Net Primary Production (NPP) in g C/$m^2$/day at eight depths in the water column in the Urania Basin during 2005/2006.

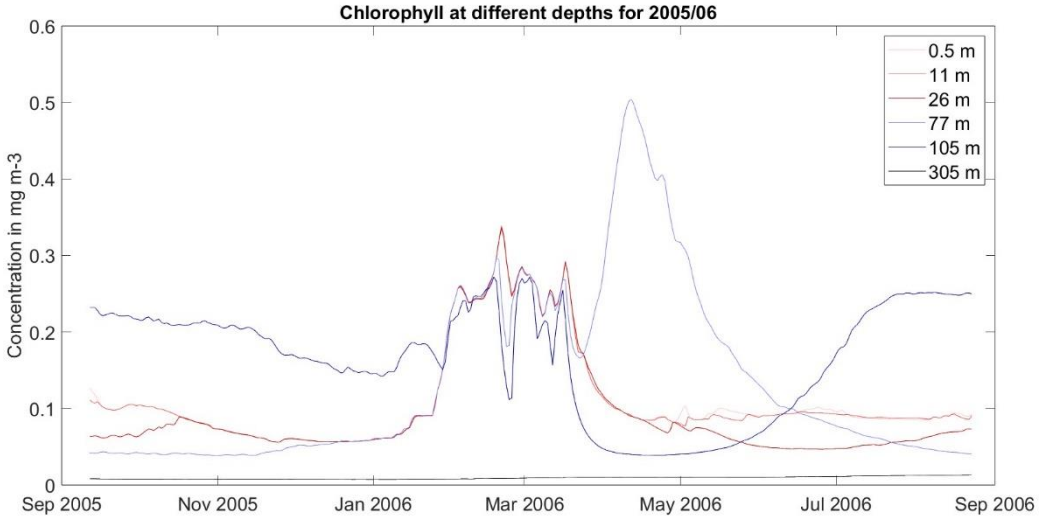


Fig. A.2: Chlorophyl concentration in mg/m$^3$ during 2005/2006 at 6 different depths in the water column (Global Ocean Biogeochemistry Hindcast)

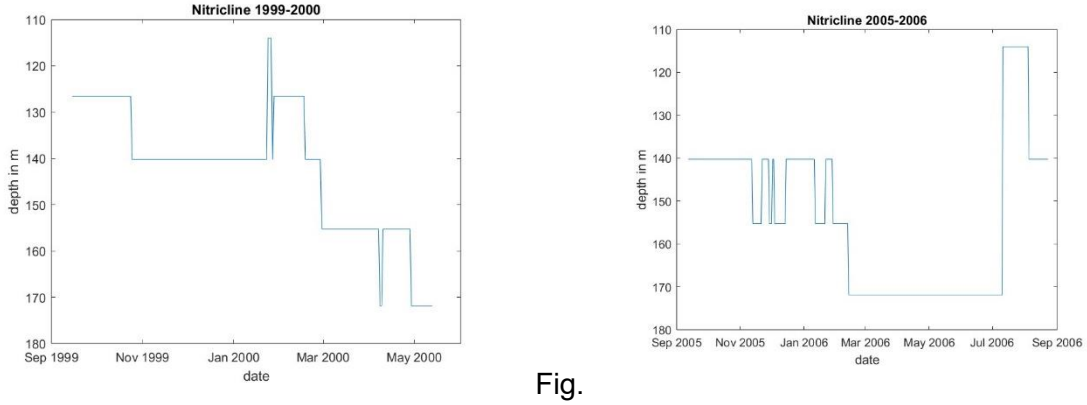


Fig.

Fig. A.3: Nitracline. The depth in the water column with the largest increase of Nitrate concentration per meter.

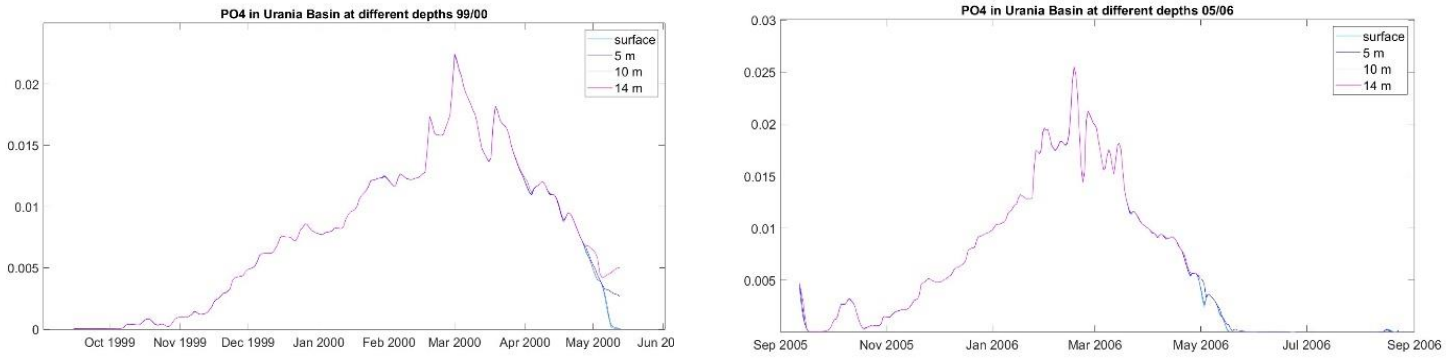


Fig. A.4: Phosphate concentration in µmol/L at 4 depths in the water column measured in the Urania Basin during both years.